



# Soil loss risk assessment of lateritic badland surface of Garhbeta Block-I, West Bengal, India using an integrated approach of Revised Universal Soil Loss Equation (RUSLE) algorithm and geospatial techniques

Anurupa Paul<sup>1</sup> · Ipsita Mallik<sup>1</sup> · Joydeb Sardar<sup>2</sup> · Jatisankar Bandyopadhyay<sup>1</sup>

Received: 14 April 2022 / Revised: 10 June 2022 / Accepted: 11 June 2022 / Published online: 2 July 2022  
© The Author(s), under exclusive licence to Springer Nature Switzerland AG 2022

## Abstract

The Pleistocene-Holocene climate change with the consequences of wet and dry conditions of the tropical humid to the sub-humid environment of the region provided a favourable site for interaction of geomorphological and active pedological processes over the lateritic bands. The study reveals that the exposure of lateritic banks up to 21 m in thickness from the river Shilabati bed indicates the down cutting process of the high energy phases of the fluvial processes in the geological past. The integrated approaches of Revised Annual Soil Loss, extensive field-based measurement, and applied techniques of Remote Sensing and GIS models were used to estimate the risk and hotspot of annual soil loss in the lateritic upland of the region. The five parameters were used in the RUSLE model as; Rainfall Erosivity(R), Soil erodibility (K), Slope Length and Steepness (LS), Land Cover and Crop Management(C), and Support Practice (P). The estimated annual average soil loss is recorded at > 7–20 ton/ha/year in the region. The multivariate regression and CDF plots were used to study the strength of the relationship between NDVI ( $R^2 = 0.859/0.722$ ;  $RMSE = 0.044$ ), BSEI, ( $R^2 = 0.84/0.722$ ;  $RMSE = 0.038$ ) and soil loss in the region. The huge amount of soil loss can be arrested by planting vegetations (i.e., Cashew Nut trees) over the remaining badland surface areas. The ecological bio-engineering methods such as “vetiver grass root plantation” directly compact the soil or sediment by their root systems to reduce soil erosion. However, these types of policymaker management practises are required to reduce soil loss in the Garhbeta lateritic badland region's steeper slopes and river basin areas.

**Keywords** Ecological bio-engineering methods · Lateritic bands · Pleistocene-Holocene climate · Pedological processes · RUSLE model

## Introduction

Soil erosion contributes to the loss of agricultural land productivity, ecological disbalance of the ecosystem, and aesthetic values of the natural environment, and it impairs the production of drinking water and hydro-energy production (Panditharathne et al. 2019). Soil erosion is the natural process of removing the upper soil materials and their transport through the action of erosive movements such as water, weathering wind velocity, and human disturbance in the environment (Gunawan et al. 2013). Agricultural land degradation is a major global phenomenon caused by the loss of surface soil nutrient concentration, increased runoff from more impermeable subsoil, and decreased water concentration in the plants (Ganasri and Ramesh 2016). The average annual soil loss erosion rate worldwide is about 30 t

---

✉ Anurupa Paul  
anurupapaul2017@gmail.com

Ipsita Mallik  
anil240262@gmail.com

Joydeb Sardar  
joydebvu@gmail.com

Jatisankar Bandyopadhyay  
jatib@mail.vidyasagar.ac.in

<sup>1</sup> Department of Remote Sensing & GIS, Vidyasagar University, Midnapore 721102, West Bengal, India

<sup>2</sup> Cente for Environmental Studies, Vidyasagar University, Midnapore 721102, West Bengal, India

ha<sup>-1</sup> yr<sup>-1</sup> ranging from 0.5 to 400 t ha<sup>-1</sup> yr<sup>-1</sup> (Pimentel et al. 1987). The rate of annual soil erosion and sediment capacity load yield is measured quantitatively and consistently with the help of two types of models: physical-based models and empirical models. In general, physical-based models are used for soil erosion control by solving various equations, but physical models are used for measuring soil erosion and estimating sediment yield from catchment areas (Bhattarai and Dutta 2007). There are several empirical, conceptual, and physical-based models widely used in suitable site selection of Soil loss estimation; e.g. the Universal Soil Loss Equation (USLE), Modified Universal Soil Loss Equation (MUSLE), and Revised Universal Soil Loss Equation (RUSLE) are the most popular soil loss erosion prediction models used globally (Wijesundara et al. 2018; Udayakumara et al. 2010; Singh and Panda 2017). In general, the U.S Department of Agriculture developed by the RUSLE model and it is used as a decision matrix support system to estimate soil conservation and land use planning (Angima et al. 2003). It is adopted as a numeric mathematical expression to describe the ecological processes related to conservation management practises and erosion in a given landscape (Agele et al. 2013). Soil erosion occurs as a result of changes in agricultural production practices, ecological disturbance of nature, agricultural intensification, land degradation, and changes in global climatic conditions (Yang et al. 2003). The RUSLE mathematical model has been adapted to estimate and predict soil loss in a river basin catchment area where the soil erosion is significant. Rill and gully erosion are the major results of the removal of surface soil particles from their parent place of origin by the raindrops (Biswas and Pani 2015; Bewket and Teferi 2009). In general, 12% of physical weathering and 4% of chemical reaction of soil leads to small amounts of soil loss (Brady and Weil 2012). Soil is mainly affected by 56% of rainwater erosion and 28% of wind erosion. (Narayana and Babu 1983) It has been estimated that in India, 16.4 t ha<sup>-1</sup> (5334 m-tonnes) of soil is eroded due to various natural and anthropogenic reasons. However, 29% of soil is eroded and carried away by the river and deposited into the sea. (Brady and Weil 2012). Soil erosion is the major problem in the river basin catchment area. It also reduces the nutrient load that can be affected in the growth of plantation and also increases in the sedimentation load of the river bank margin area. (Narayana and Babu 1983).

Gullying is a potent form of land degradation, accounting for a significant portion of the total sediment yield in river basins (Poesen et al. 2003). Lithology, climate, topography, and land use all contribute to the formation of gullies, but they occur particularly in areas where the soil is prone to forming pipes and crusts (Valentin et al. 2005). Recent reviews on badlands have emphasized the current trends in badland research, including the variability of erosion rates,

the site-specific nature of such erosion (e.g. the roles of the physico-chemical properties of the soil and biota in causing badland erosion), and modelling their long-term evolution and anthropogenic effects in badlands (Gallart et al. 2013; Nadal-Romero et al. 2018). With the help of spatial analysis techniques, the RUSLE model was developed for use as a better analyzer to assess the annual average soil loss estimation, identify the hotspot areas and evaluate possible management system measures with the help of spatial analysis techniques (Stillhardt et al. 2002; Nyssen et al. 2004; Kaltenrieder 2007; Atoma et al. 2020). A group of researchers have been studying the use of the RUSLE model to estimate annual average soil loss for various geomorphic surfaces and land-use practises on steep slopes (Renard et al. 1996; Dunn and Hickey 1998; Mekuriaw et al. 2018; Miheretu and Yimer 2018).

This is a major regional problem in the badland tract of the Shilabati river catchment areas of the western part of the Garhbeta Block-I. However, the sand mining activities in catchment areas of alluvium flood plain surface and the agricultural productivity are reduced in the region of active soil loss areas due to the impact of climate variability, physical and chemical weathering intensity in hardpan duricrust lateritic surfaces, flood hazards, and land use alterations, which cause soil nutrient deficiencies that have natural effects on local habitats and ecosystem services in the region. The present study is an attempt to focus on the estimation of annual average soil erosion (RUSLE Model) in the surrounding areas of the Garhbeta Block-I to delineate the probable soil erosion potential areas in the subtropical region and its impact on Shilabati river basin sedimentation. The study is also validated with the spectral indices of NDVI and BSI techniques, and they are statistically correlated as well as with the identification of risk probability zones, followed by field investigations in the region. However, research gaps remain in the existing research regarding, e.g., variations in the weathering intensities across the Rarh lateritic landscape over the Late Quaternary (last 1.5 million years), and the site-specific characteristics that affect the mode of soil erosion in these lateritic badland landscapes (Garhbeta). The analysis of geospatial data coupled with detailed fieldwork reveals that the Gangani tracts can be divided into two distinct zones; i.e., i) the older badland tract found in the central and eastern parts of the area and ii) the newer badland tract occupying the western part.

## Study area: geographical setup

The study area has been chosen as Garhbeta-1 Block. It is situated 4 km southeast of Garhbeta railway station in Paschim Midnapore, West Bengal, India typical humid region, very prone to shallow erosion. The erosion of rills and

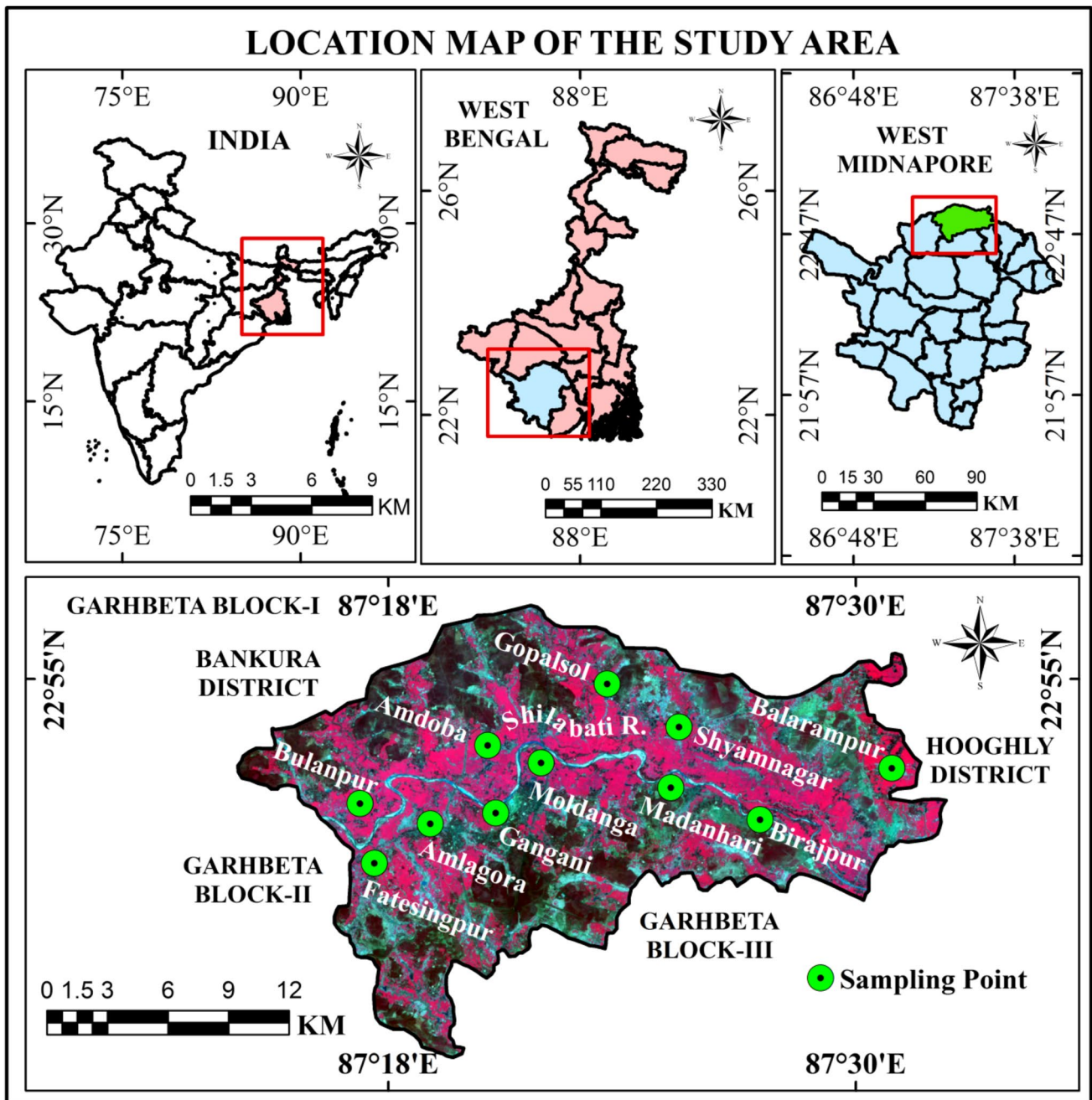


**Fig. 1** The study area of the Garhbeta Block-I (Gangani badland topography), Paschim Medinipur

gullies is also influenced by lithological conditions and topsoil in the region. The area is bounded by Bankura District in the North, Hooghly District and the Chandra Kona-I and Chandra Kona-II are located in the East, the Garhbeta-III CD Block in the South, and the Garhbeta-II CD Block in the West. The area is located 58 km from Midnapore, the district headquarters, which is located between 22°47'12" N and 22°56'27" N latitude, and 87°13'17" E to 87° 23'29" E longitude (Fig. 1). The area is covered by 3.2 km<sup>2</sup> of Pleistocene lateritic upland, and the Garhbeta Badlands belong to the

Lalgarh formation, and which is also known as the ‘Grand Canyon’ of West Bengal. The Shilabati River is the major river in this study area of Gangani. The major river channels in Paschim Midnapore, such as Kasai or Kangsabati, Rup Narayan, Subarnarekha, etc. The landscape of Gangani is morphologically quite different from the adjacent rolling plains, with active ravine erosion and a long escarpment facing the Shilabati river fringe area of the Bengal Basin. Different types of morphological features are situated in this study area, like Rills, Gully, Escarpment, Ravine, Gully Fan,

Headward Erosion, Duricrust, Cave, Braided, Alluvial Plain, Flood Plain, micro-morphological forms like pipes, mounds and pillars etc. Geologically the Shilabati Basin is diverse, comprising of residual Archaean granites that underlie the undulating pediplain in surfaces in the headwater reaches. This terrain grades into the deeply weathered duricrust zone that corresponds to the Lalgah Formation, which covers extensive parts of the basin in its south western portion. The lower floodplains towards the east and south east are covered by Quaternary alluvium.

### Geological formation & soil settings

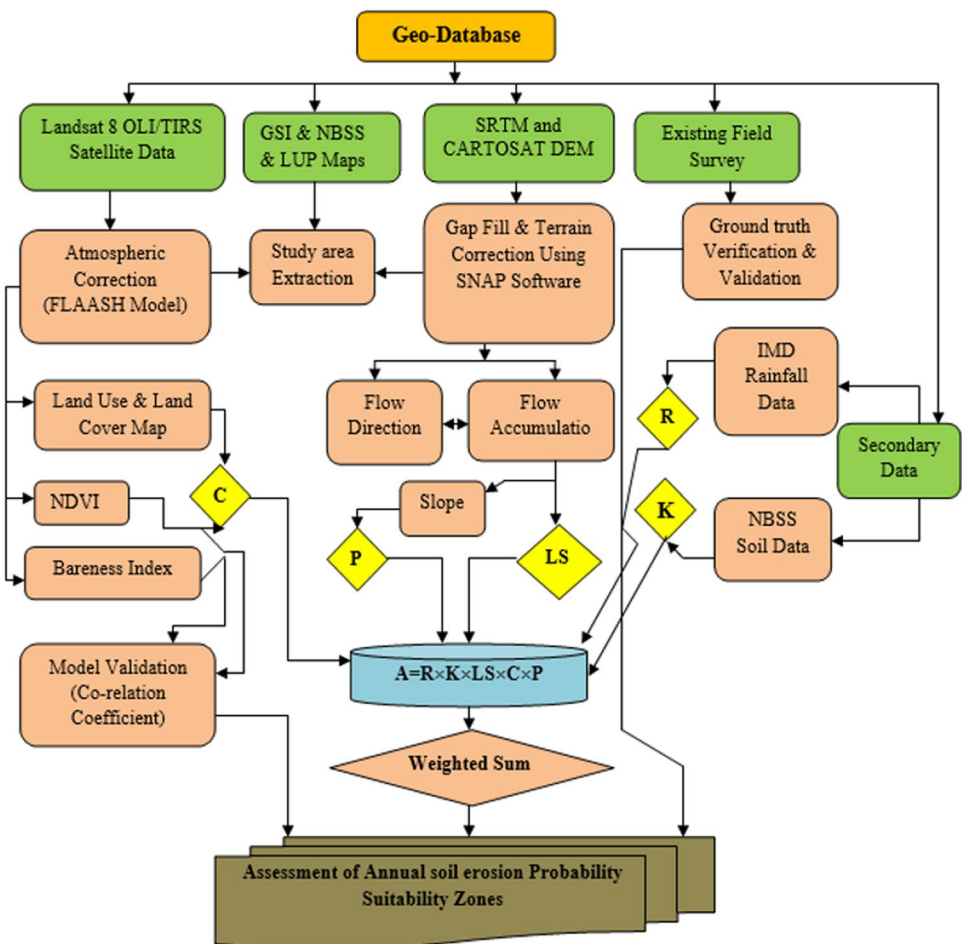
Geologically, this study area is a part of the Chhotanagpur plateau margin, the western margin of the Bengal Basin, which is extremely dissected, discontinued, and is characterized by rolling and undulating rills and gullies. In this present study area, In this present study area, two types of geology are found, which are extended in the eastern portion, covered by greenish grey clay, impregnated with caliches nodules, and the other portion is covered by fragments of quartz, phyllite, and granite pebbles with gravels occasionally lateralised. The lateritic soil heavily leaches the

subsoil; it gets dries and gets rock-like due to the cementing of ferruginous concretion by iron oxide colloid when it is exposed. In this study area, six broad soil groups are found, such as Vertisols, Inceptisols, Entisols, Oxisols, Ultisols, and Alfisols.

### Materials & methods

The current study estimates average annual soil loss in the Garhbeta Block-I (Gangani; Shilabati river basin catchment area) area using the Revised Universal Soil Loss Equation (RUSLE) in conjunction with an Arc GIS.10.3 and ERDAS. 14 image processing software interface to develop the unique methodology to estimate soil erosion hazard map of the lateritic badland topography region of Gangani Danga (Fig. 2). With the help of different algorithm analyses, the factor maps were selected on the basis of their significance and importance for soil loss estimation. Soil erosion of lateritic badland topography is estimated through different empirical and physical algorithm-based models. The present study was conducted because the soil erosion

**Fig. 2** Methodology of the flow chart describing the overall procedure adopted to identify the average soil loss erosion (AVSL) in the Study area





has been generated with the help of the RUSLE model (Renard et al. 1991; Millward and Mersey 1999; Wen et al. 2015). However, many models have been adopted and developed by a bunch of research scholars to estimate soil loss erosion, like EUROSEM (Morgan et al. 1998), LISEM (De Roo et al. 1996), SWAT (Arnold and Fohrer 2005), and WEPP (Flanagan et al. 2007). In general, the vector layer as a soil map (Fig. 5) was converted into a raster layer with the help of the ARC GIS 10.3 platform, and the raster layers such as; Rainfall (Fig. 4), Flow accumulation grid (Fig. 6), Land use and Land cover (Fig. 7), Slope (Fig. 8), and NDVI (Fig. 11a), were reclassified by using the weighted sum method. The all factor map has

been reclassified into different categories for the purpose of the significant level. The factor map has been estimated into 1 to 5 ranks in different aspects, where rank 1 has the least significance and rank 10 has more significance for a suitable site selection in the hotspot of a particular region (Fu et al. 2006). Basically, the USLE/RUSLE model is a coefficient that is calibrated on the basis of observations of soil erosion, and it cannot measure the actual soil loss. However, it is widely applicable because of its data availability. (Jain and Kothiyari 2000; Bhattarai and Dutta 2007; Pandey et al. 2007; Sinha and Joshi 2012; Balasubramani et al. 2015) (Figs. 3, 4, 5, 6, 7, 8, 9, 10, and 11).

**Fig. 3** Mean Annual Rainfall distribution of Garhbeta Block-I, 2013 to 2017(IMD)

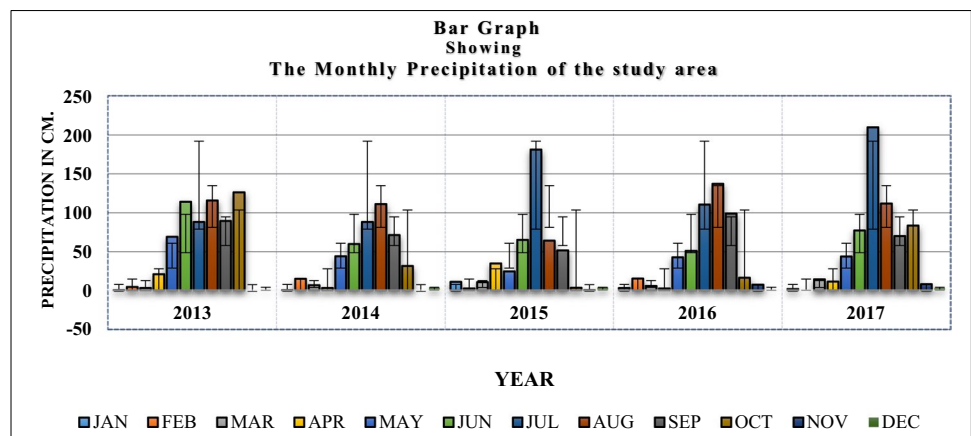


**Fig. 4** Rainfall erosivity factor map (R factor)

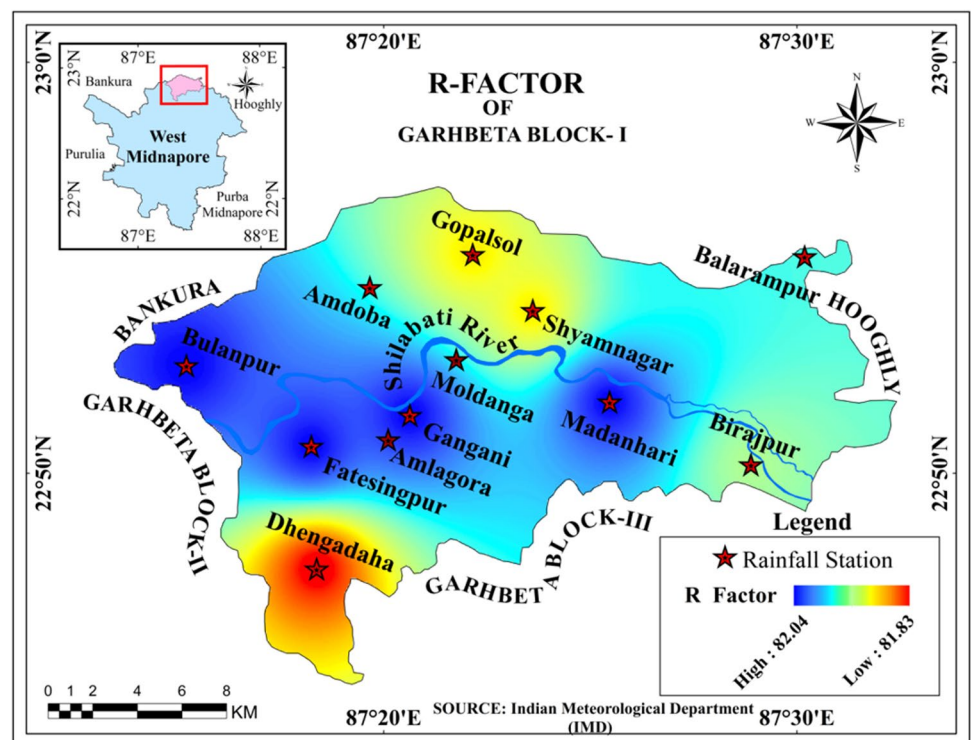
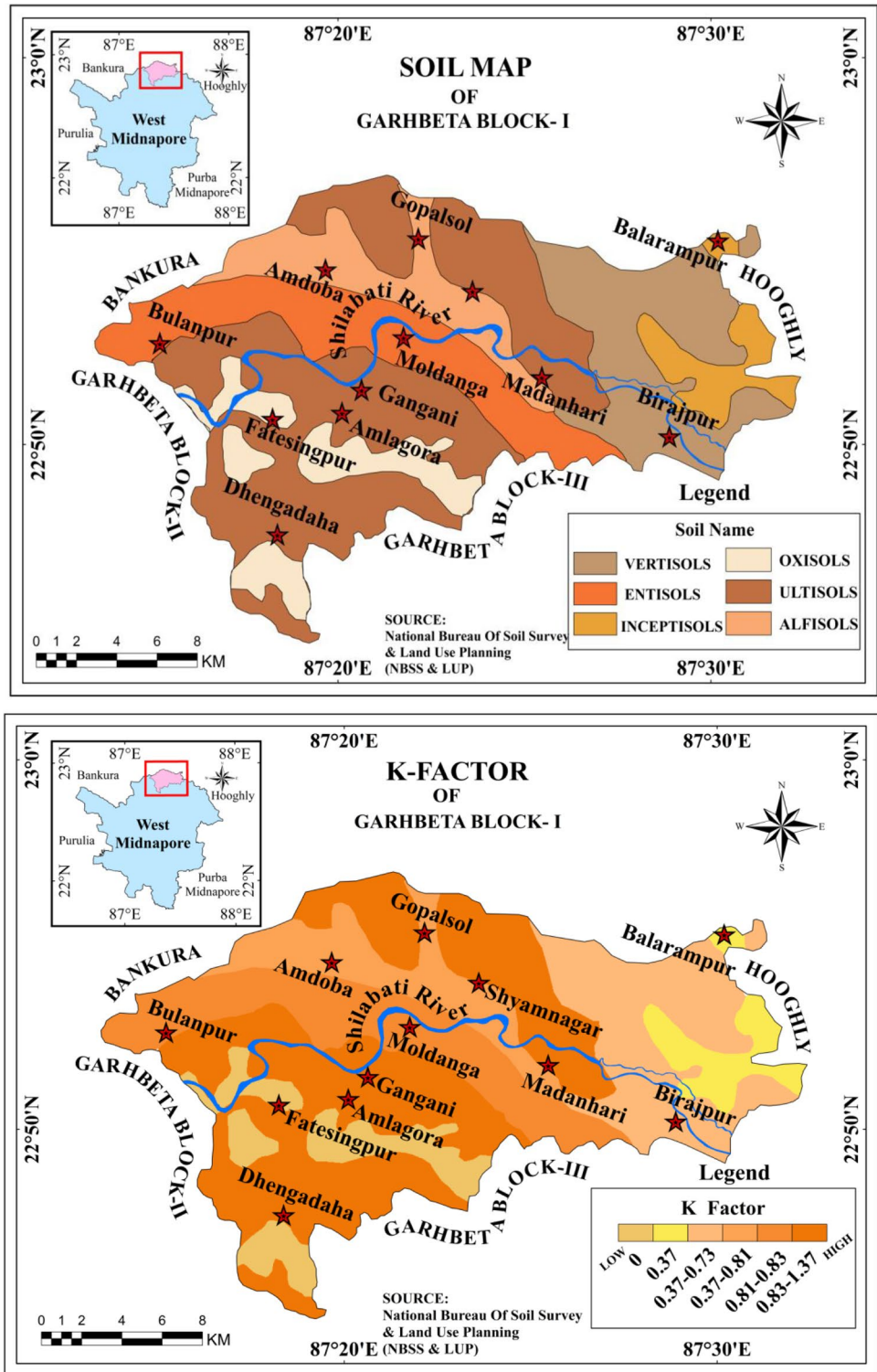


**Fig. 5** Soil map and Soil erodibility factor map (K)

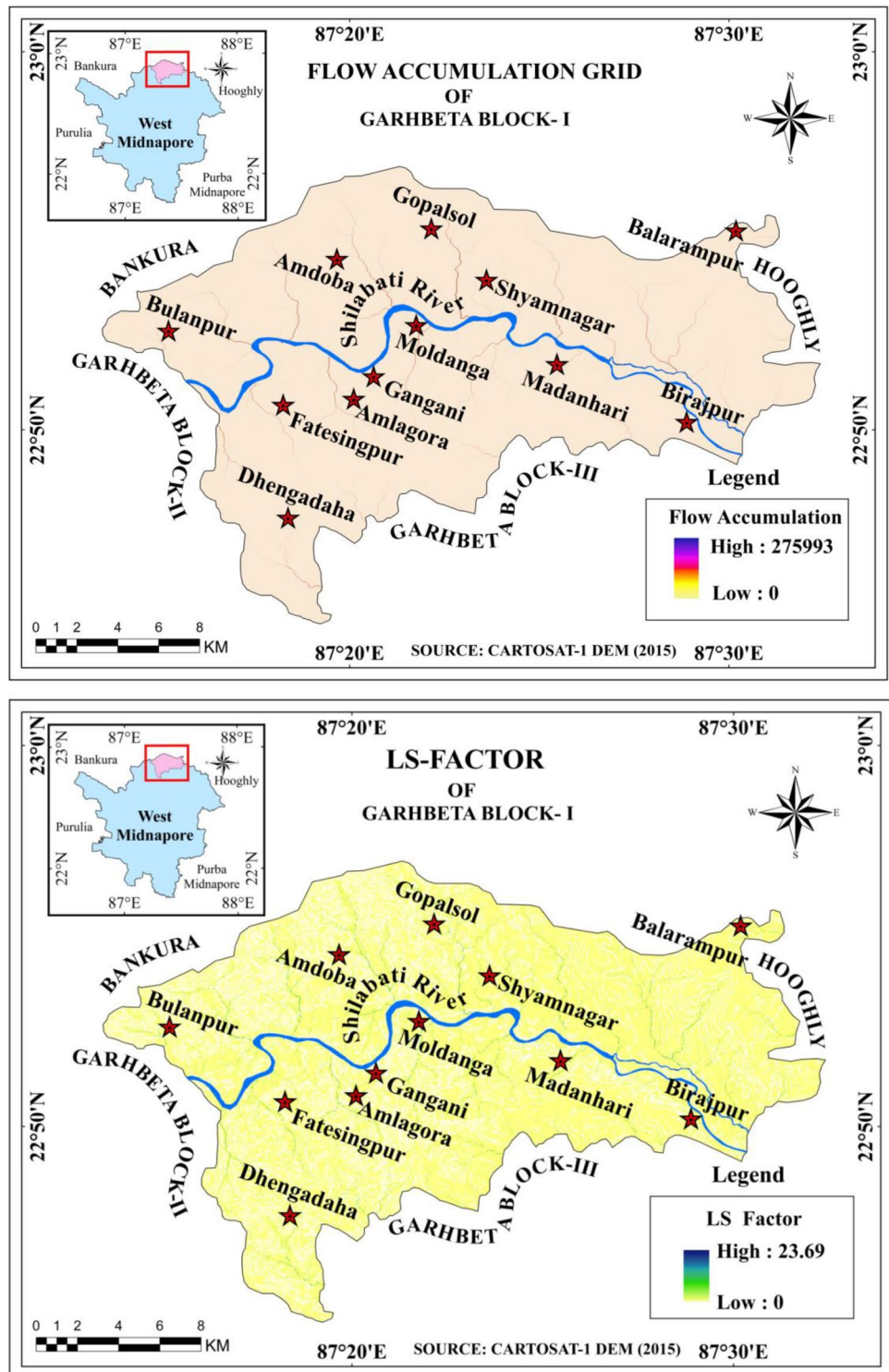


**Data used**

The Landsat 8 OLI/TIRS data (LULC, NDVI, and BES1), soil data (NBSS&LUP), CARTOSAT & SRTM DEM (Slope), geology map, and also field-based

measurement (ground truth verification) were used to extract the outcome of the present study area (Table 1). All the statistical regression analyses and plots were performed using the XLSTAT package at  $\alpha = 0.05$  confidence level.

**Fig. 6** Flow accumulation map and Land management support factor (LS)



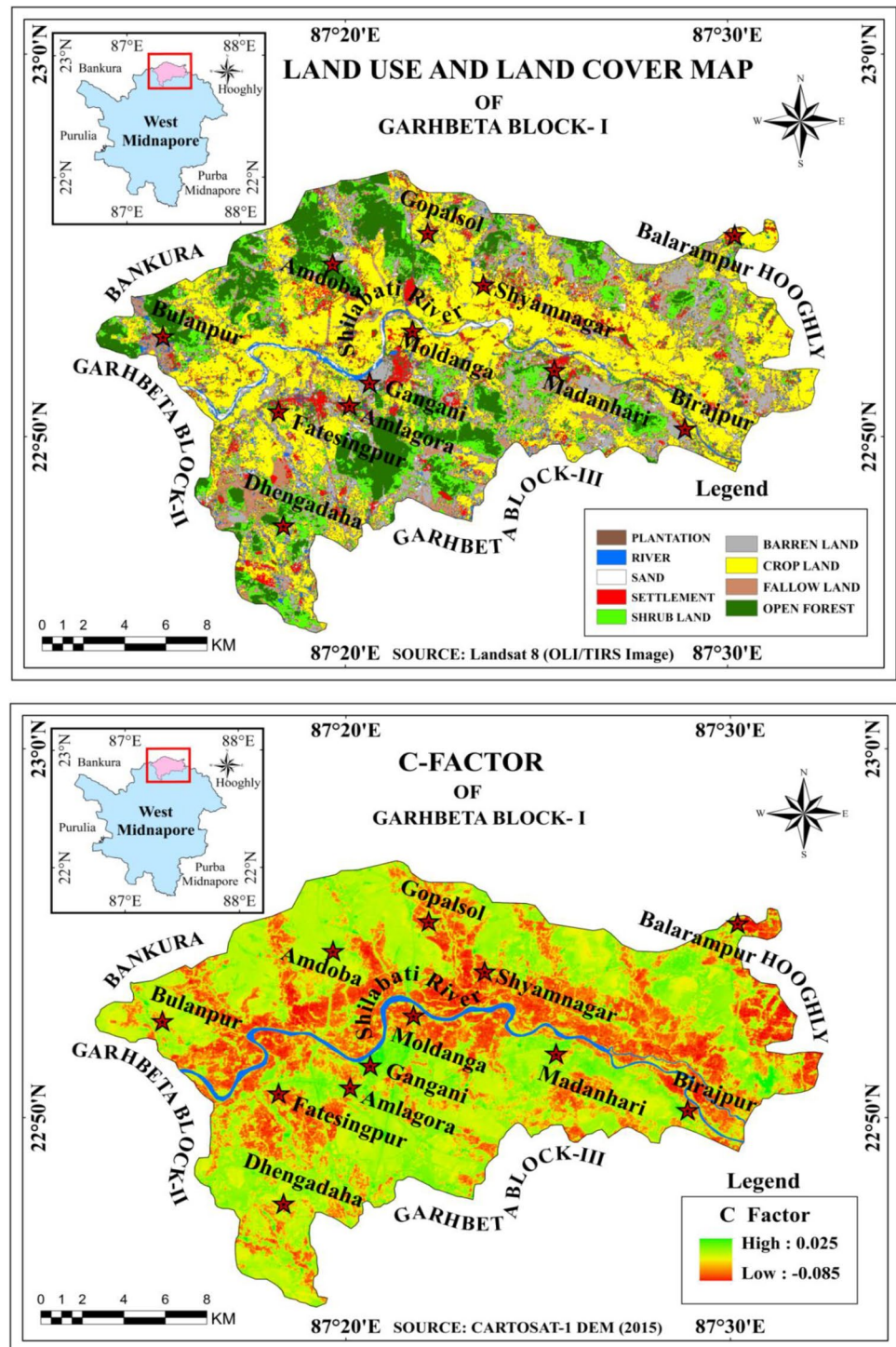
**Metrological condition**

The rainfall data is collected by the Indian Meteorological Department, India (IMD). The rainfall data has been collected from 9 sampling stations for the years 2013 to

2017(Fig. 3) to gain an understanding of the change in the climatic conditions. The highest rainfall is recorded at 209.9 cm in the month of July and the lowest precipitation is 10 cm in the month of February in 2017.



**Fig. 7** Land Use and Land cover (LULC) with Crop management factor(C)



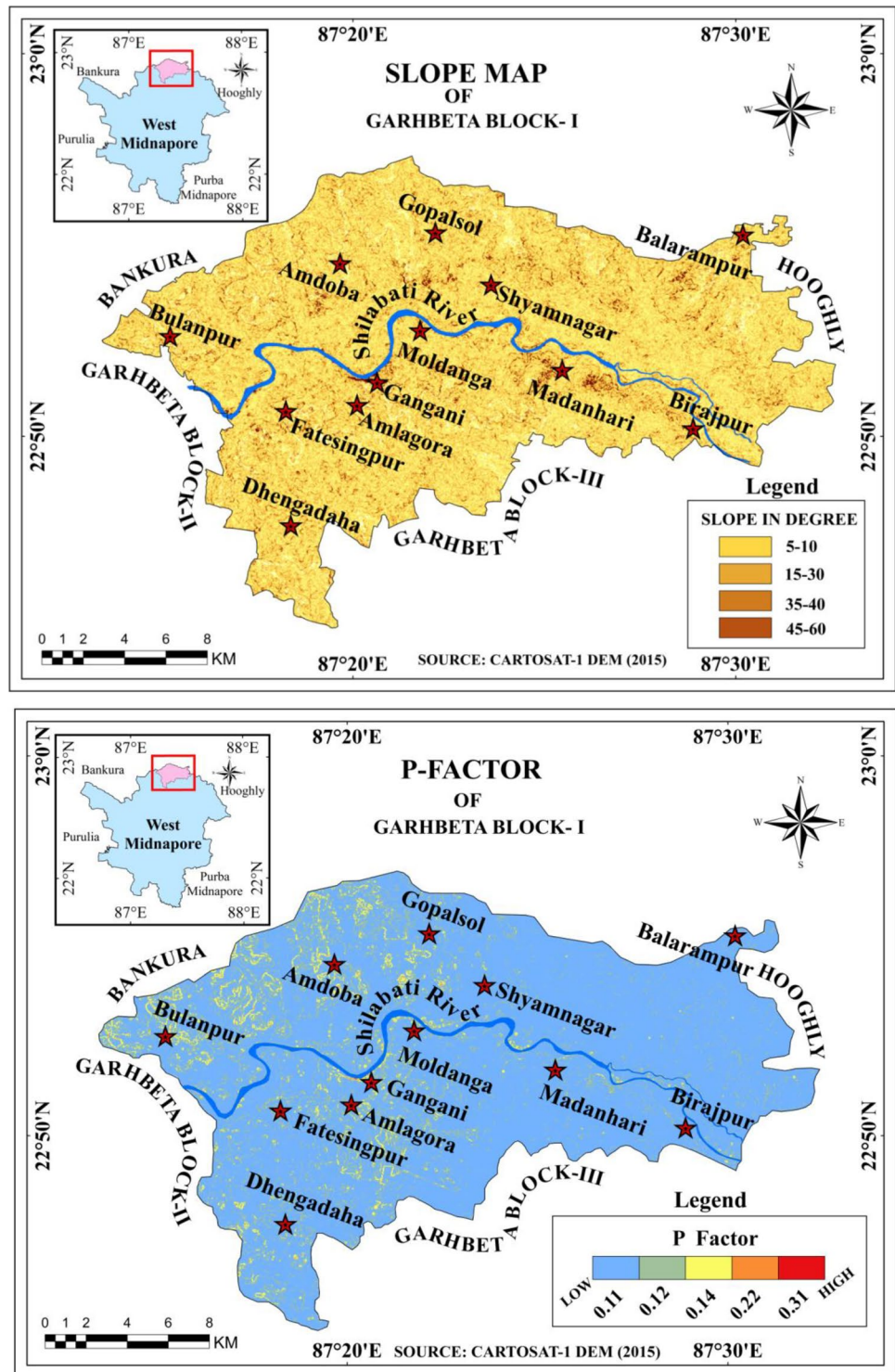
### Soil loss estimation parameters (RUSLE Model)

The amount of soil eroded at a specific time over an area is called net soil loss. It is expressed in the unit area (ton ha<sup>-1</sup> y<sup>-1</sup>). The calculation of annual average soil loss for

Gangani Badland topography (Garhbeta Block-I) is performed using (RUSLE) the Revised Universal Soil Loss Equation Mathematical Algorithm and it was interfering with the ArcGIS 10.3 Platform. The primary equation of the RUSLE model (Renard 1997) is generally (Eq. 1) expressed as follow,



**Fig. 8** Slope map and Support factor map (P)



$$A = R * K * LS * C * P \tag{1}$$

where, average annual soil loss (metric t/ha/year), R rainfall erosivity factor (Mega Joules mm per h/ha/year). K soil erodibility factor (metric t/ha/MJ/mm), LS slope length

steepness factor (dimensionless), C cover and management factor (dimensionless), and P erosion support practice or land management factor (dimensionless). The RUSLE input factors with units where, ‘MJ’ is mega joule, ‘mm’ millimetres, ‘ha’ hectares, ‘yr’ years and ‘t’ tons (Renard 1997).

**Table 1** Factor map for annual average soil loss erosion estimation and description different types of Geo-spatial & Non-spatial data

Sl.No	Data Types	Data Source	Details of the data	Year
1	Landsat-8 OLI/TIRS	United States Geological Survey (USGS) site ( <a href="https://earthexplorer.usgs.gov/">https://earthexplorer.usgs.gov/</a> )	Landsat 8 Consist of two instruments one is operational Land Imager (OLI) and another Thermal Infrared Sensor (TIRS) spatial resolution of 30 m for visible, NIR, SWIR, 100 m for Thermal and 60 m for Panchromatic band	2019
2	Digital Elevation Model	United States Geological Survey (USGS) site ( <a href="https://earthexplorer.usgs.gov/">https://earthexplorer.usgs.gov/</a> and <a href="http://www.bhuvan.nrsc.gov.in">www.bhuvan.nrsc.gov.in</a> )	Shuttle Radar Topography Mission (SRTM)—1 arc-second for global coverage The Spatial resolution is 30 m and CARTOSAT-1 Spatial resolution-2.5 m	2019
3	Rainfall Data	Indian Metrological Department, India (IMD) ( <a href="https://mausam.imd.gov.in/">https://mausam.imd.gov.in/</a> )	Rainfall data for a period of 10 years (2013–2017) with 9 rain gauge stations	2013 to 2017
4	Soil Data	The National Bureau of Soil Survey and Land Use Planning, India ( <a href="https://nbsslup.icar.gov.in/">https://nbsslup.icar.gov.in/</a> )	Soil map for the year 2003. categories of soil based on the soil texture	2003

### Rainfall erosivity(R factor)

Rainfall and surface runoff play an important role in the process of soil erosion, which is basically expressed as the "R factor." The rainfall and runoff erosivity factors act as the forces for the sheet and rill erosion. A high rate of rainfall and large drop size can erode the soil particles faster than normal rainfall. Also, the high rate of runoff flow is caused by heavy storm rainfall that leads to sheet or rill erosion. The estimation of soil loss was affected by precipitation and surface runoff conditions of sub-surface soil, which was influenced by the rainfall erosivity factor (Yue-Qing et al. 2008). Therefore, the annual rainfall variability and rainfall erosivity factor map of Gangani (Shilabati river basin); which have been generated on the basis of interpolating mean annual rainfall based on Semivariogram IDW (Inverse distance weighted) techniques with the help of the ARC GIS 10.3 platform. According to the cross-validation results, IDW provides the least error (RMSE 82.04) for mapping rainfall data (Table 2). The general equation for the IDW method (Eq. 2) is expressed as (Chang 2018).

$$z_0 = \frac{\sum_{i=1}^s z_i \frac{1}{d_i^k}}{\sum_{i=1}^s \frac{1}{d_i^k}} \quad (2)$$

where,  $z_0$  is the estimated value at point 0,  $z_i$  is the  $z$  value at known point  $i$ ,  $d_i$  is the distance between point  $i$  and point 0,  $s$  is the number of known points used in estimation, and  $k$  is the specified power.

The empirical equation that estimates Fournier Index and R-value from annual total rainfall was used (Eqs. 3, 4, and 5) and see Table 2 below. It is given (KICT 1992) as,

$$R = \frac{1}{n} \sum_{i=1}^n \left[ \sum_{k=1}^m KE(I_{30}) \right] \quad (3)$$

where,  $KE$  is the total Kinetic energy ( $\text{MJ ha}^{-1}$ ),  $I_{30}$  is the maximum intensity of 30 min rainfall ( $\text{mm h}^{-1}$ ) given by Renard and Freid (1994).

$$F = \frac{\sum_{i=1}^{12} P_i^2}{\sum_{i=1}^{12} P} \quad (4)$$

**Table 2** Estimation of R factor in assigned in mean annual rainfall data (IMD, 2013–2017)

Sl. No	Location	Slope (in Degree)	Latitude	Longitude	R-Factor
1	Amdoba	30	22°47'41.34"	87°18'23.26"	81.83
2	Gangoni	5	22°50'40.00"	87°18'14.76"	82.04
3	Amlagora	10	22°51'25.14"	87°20'37.89"	82.04
4	Moldanga	5	22°51'44.52"	87°25'27.94"	82.04
5	Shyamnagar	5	22°50'12.90"	87°28'53.09"	81.94
6	Gopalsol	30	22°55'16.83"	87°30'11.17"	81.97
7	Dhengadaha	25	22°55'20.03"	87°22'9.15"	81.9
8	Madanhari	35	22°52'37.76"	87°15'13.31"	82.04
9	Birajpur	15	22°53'58.40"	87°23'36.34"	81.9

where,  $P_i$  is the average rainfall (mm),  $I$  is the month and  $p$  is the annual average rainfall (mm)

$$R = 38.5 + 0.35 \times Pr \tag{5}$$

where,

$R$  Rainfall erosivity factor and

$Pr$  Annual precipitation of the study area

### Soil erodibility (K factor)

The soil erodibility ( $K$ ) factor refers to the inborn sensitivity of the soil to erosion, and it depends on the physical, mineralogical, chemical, and morphological attributes of soils (Pérez-Rodríguez et al. 2007). The  $K$  factor signifies that the amount of soil loss per unit of eroded with the effects of rainfall energy during it is also removed by 9% of bare soil (Brady and Weil 2012). The soil texture, soil types, soil structure, organic matter, and permeability determine the erodibility of a particular soil. Soil organic matter reduces erodibility. Soil erodibility was a flexible factor, and it contained different organic content, types of soil, and textures (Robert and Hilborn 2000), as shown below (Table 3). Soil types and textures have been classified according to the classification provided by the United States Department of Agriculture (USDA). The soil types,

**Table 3** Different types of soil texture classes are specifically distributed the soil organic matter (Robert and Hilborn 2000)

Texture Class	Organic Matter Content		
	Average	<2%	>2%
Clay	0.22	0.24	0.21
Clay Loam	0.30	0.33	0.28
Coarse Sandy Loam	0.07	0.07	0.07
Fine Sand	0.08	0.09	0.06
Fine Sandy Loam	0.18	0.22	0.17
Heavy Clay	0.17	0.19	0.15
Loam	0.30	0.34	0.26
Loamy Fine Sand	0.11	0.15	0.09
Loamy Sand	0.04	0.05	0.04
Loamy very Fine Sand	0.39	0.44	0.25
Sand	0.02	0.03	0.01
Sandy Clay Loam	0.20	0.20	0.20
Sandy Loam	0.13	0.14	0.12
Silt Loam	0.38	0.41	0.37
Silt Clay	0.26	0.27	0.26
Silt Clay Loam	0.32	0.35	0.30
Very Fine Sand	0.43	0.46	0.30
Very Fine Sandy Loam	0.35	0.41	0.33

texture, and organic matter content have been identified with the help of district-level maps and information provided by the National Bureau of Soil Survey and Land Use Planning (NBSS) (1:50,000); Regional Centre, Kolkata (ICAR). In this study area, six types of soil classes have been identified, and their  $K$  values are assigned to different soil classes; see the table below (Table 4). The calculation is estimated through the (Eq. 6) experimental equation (Wischmeier and Smith 1978).

$$K = 2.1 \times 10^{-4} (12 - a) \times M + 3.25 \times (b - 2) + 2.5 \times (c - 3) / 100 \tag{6}$$

where,

$M$  Particle Size Parameter; (Percent Silt + Percent very fine Sand) (100-Percent Clay),

$a$  Percent Organic Matter,

$b$  Soil Structure Code used in Soil classification; and  $c$  = Soil permeability Class.

### Slope length and steepness (LS factor)

Topography plays an important role in soil erosion and landslides (Kim 1992). The  $LS$  factor represents the ratio of soil loss under a given condition. The steeper and the longer the slope, the higher the risk for soil erosion. The  $L$  factor (slope length) is defined as the outcome of the research as the distance from the source of runoff to the point where deposition begins. The  $LS$  factor has been generated using the CARTOSAT and SRTM DEM (2015) with the help of Arc GIS 10.3 and SNAP software by using gap-fill generation and also fishnet methods to extract the elevation to study the nature of the slope in this region, which has been collected by the USGS Earth Explorer. The  $LS$  factor is also known as the topographic factor. The  $LS$  factor equation is basically based on the existing conditions, including surface cover at the site. The  $LS$  factor grid was (Eqs. 7, 7.1, 7.2, 7.3, and 8) estimated with the help of this equation, which was proposed by (Moore and Burch 1986; McCool et al. 1987).

$$L = \left( \frac{\lambda}{22.13} \right)^m \tag{7}$$

where,  $L$  is slope length factor;  $\lambda$  is the field slope length (m);  $m$  is the dimensionless exponent that depends on slope steepness. 22.13 is the RUSLE unit plot length (m)

$$S = 10.8 \sin \theta + 0.03 \text{ if } \theta \leq 5^\circ \tag{7.1}$$



**Table 4** K factor value are based on the soil texture, particle size parameter (M), organic Matter (%-A), permeability classes(C), & soil structure (b)

Soil Name	Sand (%)	Silt (%)	Clay (%)	Particle Size Parameter (M)	Organic Matter %(A)	Permeability Class (c)	Soil Structure Class (b)	K-Factor
Coarse Sandy Loam	72	23	5	9025	0.07	0.75	3	0.55
Fine Sand	92	6	2	9604	0.08	1	2	0.92
Fine Sandy Loam	87	10	3	9409	0.18	2	3	0.72
Loamy Fine Sand	52	20	28	5184	0.11	1	2	0.72
Loamy Sand	80	5	15	7225	0.04	1.2	2	0.27
Sandy Clay	75	20	5	9025	0.2	1.5	2	0.55

$$S = 16.8 \sin \theta - 0.5 \text{ if } \theta > 5^0 \quad (7.2)$$

$$S = 21.91 \sin \theta - 0.96 \text{ if } \theta \leq 10^0 \quad (7.3)$$

where, S is slope steepness factor and  $\theta$  is slope angel in degree.

$$\begin{aligned} LS = & \text{Power}([\text{Flow Accumulation}] \\ & \times [\text{Cell size}]/22.13)0.4 \times \text{Power}(\text{Sin}[\text{Slope Grid}(\text{Degree})]) \quad (8) \\ & \times 0.01745/0.0896)1.4 \times 1.4 \end{aligned}$$

As the hill slope gradient increases, the velocity and the erosivity of Runoff increase. The length of the slope is longer than the amount of runoff is also higher and the steeper the slope the higher the runoff velocity which contributes to erosion. (Ustun 2008).

### Land cover and crop management(C factor)

The C Factor is the most significant value for crop management. The effect of cropping and management practises on soil erosion rates high in agricultural lands is also indicated in C Factor (Karaburun 2010). Most of the study area is public land used primarily for recreational purposes. The vegetation cover protects the soil from erosion by dissipating the raindrop energy before it reaches the soil surface. Basically, the ranges of the C factor depend on the vegetation type, canopy cover percentage, and growth development at different stages in vegetation, (Gitas et al. 2009; Rao 1981). The C factor values are assigned to a single factor of vegetation land cover, based on the land use and land cover classification (Table 5), and the modified C factor equation (Eqs. 9 and 10) was proposed by Van der Knijff et al. (2000).

$$C = 1.02 - 1.21 \times \text{NDVI} \quad (9)$$

$$C = \exp \left[ -a \frac{\text{NDVI}}{(2b - \text{NDVI})} \right] \quad (10)$$

where, a and b are unit less parameters that determine the shape of the curve relating to NDVI and C factor.

The crop management factor (CMF) was prepared on the basis of the land use and land cover map of the study area. For the image classification of land use and land cover, a satellite image has been used and it is also collected by USGS Earth Explorer (Landsat 8 OLI/TIR, 2019). The land use and land cover have been generated by supervised classification techniques using ERDAS Imagine image processing software (Joshi and Nagare 2009). The land use and land cover of the Gangani were classified into nine categories, namely, plantation, river, sand, settlement, shrub land, barren land, crop land, fallow land, and open forest. The land use and land cover maps were reclassified on the basis of the C value to regenerate the C factor map. The C-values were used in the present study, proposed by (Kim et al. 2005). The crop management factor (C) values vary between 0 and 1 which is basically based on the types of land cover.

### Support practice (P factor)

The support practice factor (SPF) is a measure based on the cultivation method. It is a measure of the relationship between contouring and slope in cultivated crop field areas (Pandey et al. 2007). There are contour, Cropping, and terrace as its methods and it is an important factor that can control erosion. The P values have been calculated based on the cultivation method. The P-values range from 0 to 1. Where the value of 0 means a very good manmade erosion resistance facility and the value of 1 represents no manmade erosion resistance facility (Simms et al. 2003). The support practice factor was assigned according to the cultivating methods and aspect of a slope (CARTOSAT and SRTM DEM); it is given by Yang et al. 1999 (Table 6).

**Table 5** Crop management factor (C) for assigned in different types of Land Use & Land Cover types

Sl. No	Land Use & Land Cover	Area in Hectares	Area (%)	Ranges of C Factor
1	Open Forest	6422.4	17.856651	0.008
2	Shrub Land	8274.69	23.006704	0.014
3	Plantation	363.24	1.009942	0.02
4	Fallow Land	5157.63	14.340122	0.33
5	Crop Land	11,657.25	32.411474	0.28
6	Settlements	1633.77	4.542486	0.09
7	Barren Land	1928.88	5.363001	1.0
8	River	391.32	1.088015	0.0
9	Sand	137.25	0.381606	0.01

**Model validation**

The Normalized Difference Vegetation Index (NDVI) is directly related to ground parameters such as vegetation phenological health assessment, photosynthetic activity of the plant, leaf area index, and the amount of biomass in the particular area (Fig. 11a). NDVI values range from + 1.0 to -1.0. Areas of barren rock, sand, or snow usually show very low NDVI values (0.1 or less). Sparse vegetation such as shrubs, grasslands or senescing crops results in moderate NDVI values (approximately 0.2 to 0.5). High NDVI values (0.6 to 0.9) correspond to dense vegetation. The equation (Rouse et al. 1974) is given below (Eq. 11).

$$NDVI = \frac{(\rho NIR - \rho R)}{(\rho NIR + \rho R)} \tag{11}$$

The Bare Soil Index or Bare Earth Soil Index (BSI/ BESI) was calculated to identify the difference between agriculture and non-agriculture vegetation. Bare soil is an indicator of the normalized index in the soil reflectance (Fig. 11b). The short-wave infrared and the red band are used to quantify the soil mineral composition and soil moisture content, while the blue and near-infrared spectral bands enhance the presence of vegetation (Chen et al. 2004). This index is calculated using this equation (Eq. 12)

$$BESI/BSI = \frac{(SWIR2 + R) - (NIR + B)}{(SWIR + R) + (NIR + B)} \tag{12}$$

The Root Mean Square Error (RMSE) is the uncertainty of the predicted error of standard deviation. However, it measures the residual of all data points that depends on how far from the linear regression line of all data in any predicted model, and the R<sup>2</sup> is the metric that measures where the dependent and independent variables have explained the proportion of variance in the predictive model (Eq. 13).

$$RMSE = \sqrt{\frac{\sum_{i=1}^N (P_i - O_i)^2}{N}} \tag{13}$$

RMSE measured absolute error between observed soil loss and vegetation indices to reflect the nature of the correlation. Where P<sub>i</sub> is the model value (NDVI & BSI) and O<sub>i</sub> is the observed value (Soil loss training data sets) and N is the number of observations (test sapling data sets).

**Results**

**Rainfall erosivity(R factor)**

R factor represents the driving force of sheet and rill erosion by rainfall and runoff (Naqvi et al. 2013) processes of the earth surface. The present study shows that the value of the R factor also varies according to rainfall distribution. The range of the rainfall erosivity factor (REF) is 81.83 to 82.04 MJ mm ha-1 yr-1 of the Garhbeta Block-1 (Fig. 4). The results showed that the R-value ranged between the highest values being in the middle portion (Bulanpur, Amlagora, Gangani, Madanhari, Fatesingpur & Moldanga, and surrounding areas of the Shilabati river basin catchment areas, and the lower values being observed in the northern and southwestern parts of the present study areas (Gopalsol & Dhengadaha).

**Table 6** Support Practice (P Factor) are classified in different types of slope steepness measurement (SRTM DEM)

Sl. No	Slope in(%) by Yang et al. 1999	Estimated in DEM (Degree)	P factor
1	0–5	0–5	0.11
2	5–10	5–10	0.12
3	10–20	15–30	0.14
4	20–30	30–40	0.22
5	30–50	45–60	0.43

### Soil erodibility (K factor)

Soil Erodibility Factor (SEF) values were assigned to respective soil types, texture, and organic matter in the soil of the Garhbeta Block-1 (Fig. 5). In general, the K-factor is integrated with respect to the effects of rainfall, surface runoff, and infiltration rate on soil loss, accounting for soil property influences on soil loss (Xu et al. 2005). The soil erodibility factor (k) estimates the susceptibility of soil particles or surface materials to transportation by the main agent of rainfall. The soil structure, texture, organic matter content, and permeability also contribute to the soil erodibility factor. The K value varies from 0 to 1.37 in the present study area. The results showed that the soil erodibility values for the lateritic badland areas in the middle part of the Shilabati river basin and the surrounding northwestern parts of the older badland tract of the Gangani were better than those in other lateritic areas, including the southeastern sides of the Birajpur and Balarampur. The least significant K values are associated with the lateritic soil having low moisture content, low permeability, and nutrient capacity.

### Slope length and steepness (LS factor)

The LS factor is also known as the topography factor (SLF), and this factor represents the influence of slope length and steepness on removing the topsoil. The LS factor was developed using both the raster grid accumulation and maximum downhill slope methods. Many kinds of research scholars have used these two factors, L and S, as a combined LS factor (Pal and Shit 2017). However, the high LS values illustrate the high potential for soil erosion in this area. In this study, it was observed that the minimum value of LS is 0 (north and southwestern parts) and the maximum values are 23.69 (middle portion of Shilabati river basin area). The lower LS values lead to a negative impact on the existing soil loss in the lateritic upland areas of the older badland tract (Fig. 6). The slope shape, defined by the interaction of angle and length of the slope, has an effect on the magnitude of erosion.

### Land cover and crop management (C factor)

The C Factor is the crop or land cover management factor and measures the combined effect of all the interrelated vegetation cover and management variables. The amount of protective coverage of crops on the surface of the soil influences the soil erosion rate. The C value is equal to 1 when the land has continuous bare fallow and has no coverage (Fig. 7). The C value is lower when there is more coverage of a crop on the soil surface, resulting in less soil erosion. The C factor values varied from 0 to 0.025 of the study areas. The study area has been classified into nine land use

and land cover classes. The C factor (crop management) was assigned to different types of land-use patterns using the C values given in Table 5. Basically, the land use-land cover map, NDVI and the C factor value are used to prepare the crop management factor map (Zhou et al. 2008).

### Support practice (P factor)

In RUSLE, the support practice factor is generally applied to distributed lands and represents how surface and management practices such as contouring, terracing, and strip cropping are used to reduce soil erosion (Dabral et al. 2008). The P factor value varies from 0.003 to 1; when the p-value is 0.033, which shows good protection practices, and on the other hand, the value close to 1 shows bad protection practices. The support practice factor (P) represents the impact of support practice on soil erosion rates (Fig. 8). The characteristics of the topographic scenery are that the slope ranges from 5° to 45°. Variable high soil erosion is observed in the north-western and south-western parts with slopes ranging from 35° to 45°, while moderate to low soil erosion is observed in the east and south-eastern parts with slopes ranging from 5° to 15°, respectively. The P-factor values varied from 0 to 0.31 in the present study.

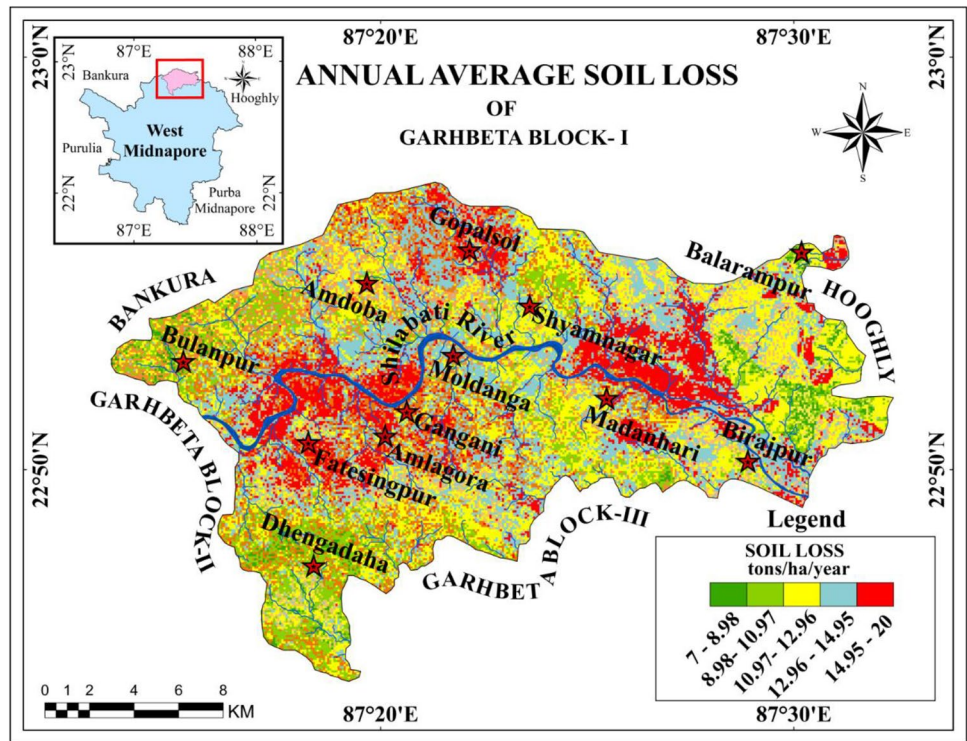
## Discussion

### Delineation of soil erosion probability zones

Several research methodologies were used by a group of researchers to calculate the main factors (R, K, LS, C, & P) for contributing to soil loss, which is the key component of the RUSLE model for estimating annual average soil loss (Renard et al. 1996; Wischmeier and Smith 1978; Hurni 1985; Poesen et al. 2003). The Annual Average Soil Loss map was created by cell-to-cell multiplication of the input raster layer in thematic maps (soil erodibility, slope gradient, rainfall erosivity, conservation practice, and cropping and management factors) and slope length in a GIS environment using the raster calculation method and weighted overlay analysis to estimate soil loss map. The estimated annual average soil of the Shilabati River lateritic upland zone ranges between > 7–20 ton/ha/year (Fig. 9). In the present research, a soil erosion hazard risk map has been generated through the RUSLE model for Garhbeta block I; which is a characteristic of this regions undulating topography based on extreme erosional features of the rill and gully of lateritic upland. The CDF plot represents the probability of the random factor as a soil loss risk area in the region. The CDF plot shows that the highly significant in the Shilabati river bank areas (high risk probability) and the less significant Bulanpur area reflect the nature of very low risk probability areas (Fig. 10).



**Fig. 9** Annual average soil loss (AVSL) probability map of the Garhbeta

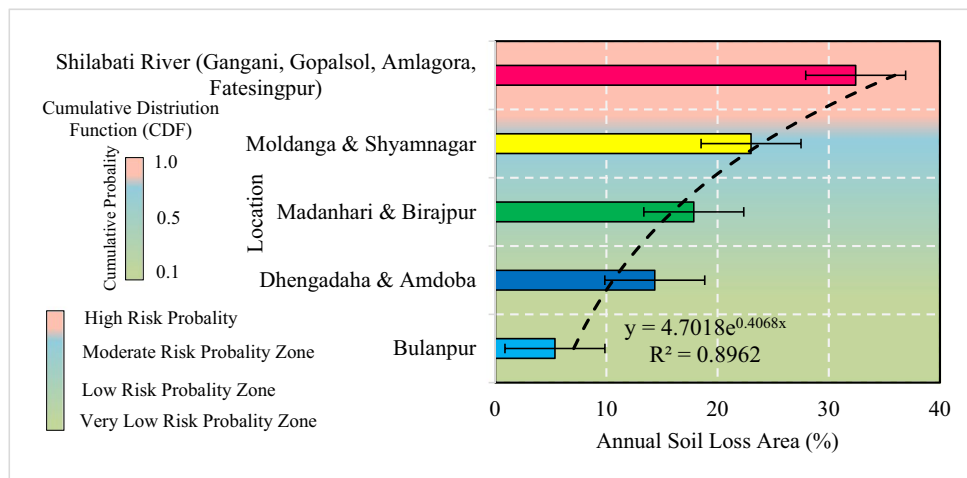


The outcome of the RUSLE model may be due to the extreme rate of soil loss (Gangani, Gopalsol, Amlagora, & Fatesingpur) being delineated as Shilabati river catchment agricultural fallow land and barren land areas (14.95 to > 20 ton/ha/year) and high erosion (Dhengadaha & Amdoba) being observed in open forest and shrubland (10.97 to 12.96 ton/ha/year) and low erosion (Bulanpur) capability rate is identified plantation or grassland areas (< 7 to 8 0.98 ton/ha/year) in Garhbeta Block I (Table 7). Remote sensing data combined with the RUSLE model in a GIS platform for determining soil erosion hazards and pinpointing high-risk prone areas where soil conservation

practises are required (Prasannakumar et al. 2011; Wang et al. 2003; Markose and Jayappa 2016).

Vetiver grass plays an important role in the sensitive nature of the hydrophytic and xerophytic characteristics as well as great physical strength, making it an ideal plant for their stabilization. Interlocking fibrous roots penetrate down to 3.0–4.5 m beneath the surface and bind soil particles while the aboveground growth extends up to a height of 1.2 m, to protect the trapping sediments, soil erosion, river bank erosion, control the high-velocity water flows and surface runoff processes, gully erosion, etc. (Grimshaw and Faiz 1995; Zeitz 2015; Yinglun

**Fig. 10** Frequency distribution of the soil erosion risk probability zone by using CDF plot



2018). It grows luxuriantly in regions receiving annual rainfall of between 100–200 cm, and the densely tufted grass can tolerate temperatures ranging from -14 °C to 55 °C. Vetiver grass (*Vetiveria zizanioides*) has been suggested as one of the most promising solutions to stabilize eroding banks in terms of its cost-effectiveness and long-term resilience (Okon and Babalola 2004; Tripathy et al. 2014). Vetiver grass will survive in the months submerged in the water. However, this type of management strategy should be implemented in this region to reduce soil and sub-surface nutrient loss, which also builds the resilient adaptive capacity of land in the tropical environment. Garhbeta has a humid tropical climate with summer temperatures > 40 °C and an annual rainfall of 140 cm, which is favourable for the luxuriant growth of the cashew nut trees. The older lateritic upland surfaces of Gangani, Gopalsol, Amlagora, and Fatesingpur and parts of Garhbeta Block-I are oxidised and demonstrate the colonies of terrestrial plants like *Shorea robusta sp.*, *Anacardium sp.*, and *Mangifera sp.* etc. in the form of semi-natural forest. In the absence of the cashew nut (*Anacardium occidentale*) vegetation cover, several blowout spots have been developed in the previous decades, particularly along the older lateritic upland surface by concentrated wind energies which gradually extended the rapid soil erosional activities on the southwestern part of the Shilabati river basin catchment areas. (Paul 2002). Soil erosion control is better protected in native bioengineered vetiver grasses than in cashew nut trees in the current region. The present status of the study area depicted that the soil erosion is highly arrested in the gully front areas of the older tracts (*Eucalyptus sp.*) of the lateritic upland in the region.

### Spectral indices: NDVI and BSI/BESI

The present study reveals that the inclusion of a  $\rho$ SWIR,  $\rho$ red and  $\rho$ NIR reflectance bands can provide useful complementary information on the geometrical structure of the canopy, health condition of the species, the optical properties of the underlying soil composition, soil moisture, and even

surrounding green covers, and can adjust canopy closure and background reflectance in the retrieval of the both spectral indices of the NDVI and BSI (Nguyen et al. 2021; Becker and Choudhury 1988). Vegetation cover is an essential influential factors for soil erosion that is depend on the physiographic aspects of the slope length and steepness factor (Benkobi et al. 1994) The generated data of the annual average soil loss in the study area, viz., NDVI and BSI, were utilised to study the sensitivity of the region. Bare soil index performance differs from the humid to tropical dry arid regions. The Normalized Difference Vegetation Index map of the Garhbeta Block-I showed 0.32–0.45 in the north-western and southwestern parts of the Shilabati river basin catchment areas, 0.24–0.32 in the northwestern part of the Amdoba, and the least amount ranged from -0.13–0.16 in the lateritic badland surfaces (Fig. 11a). The BSI values are recorded in May -June months, respectively, in Garhbeta Block-I due to the occurrences of moderate amounts of rainfall (1400 mm). The bare soil index ranges from 49.21–172.03 in the region. The highest amount of bare soil is recorded in the lower part of the southwestern region, and the least significant is found in the Shilabati river catchment areas (Fig. 11b). Among them, low NDVI and BSI values do not represent the healthier environment of the smaller tract of the older and newer badland region to support multiple activities like tourism-recreation, agriculture, settlements, horticulture, etc., over a long period. Overall assessment of the areas indicates the high sensitive hotspot region in the Shilabati river basin areas and the low sensitive areas in the badland tract of the Gangani. The multiple linear regression model helped to focus on the relationship between spectral indices and soil loss.

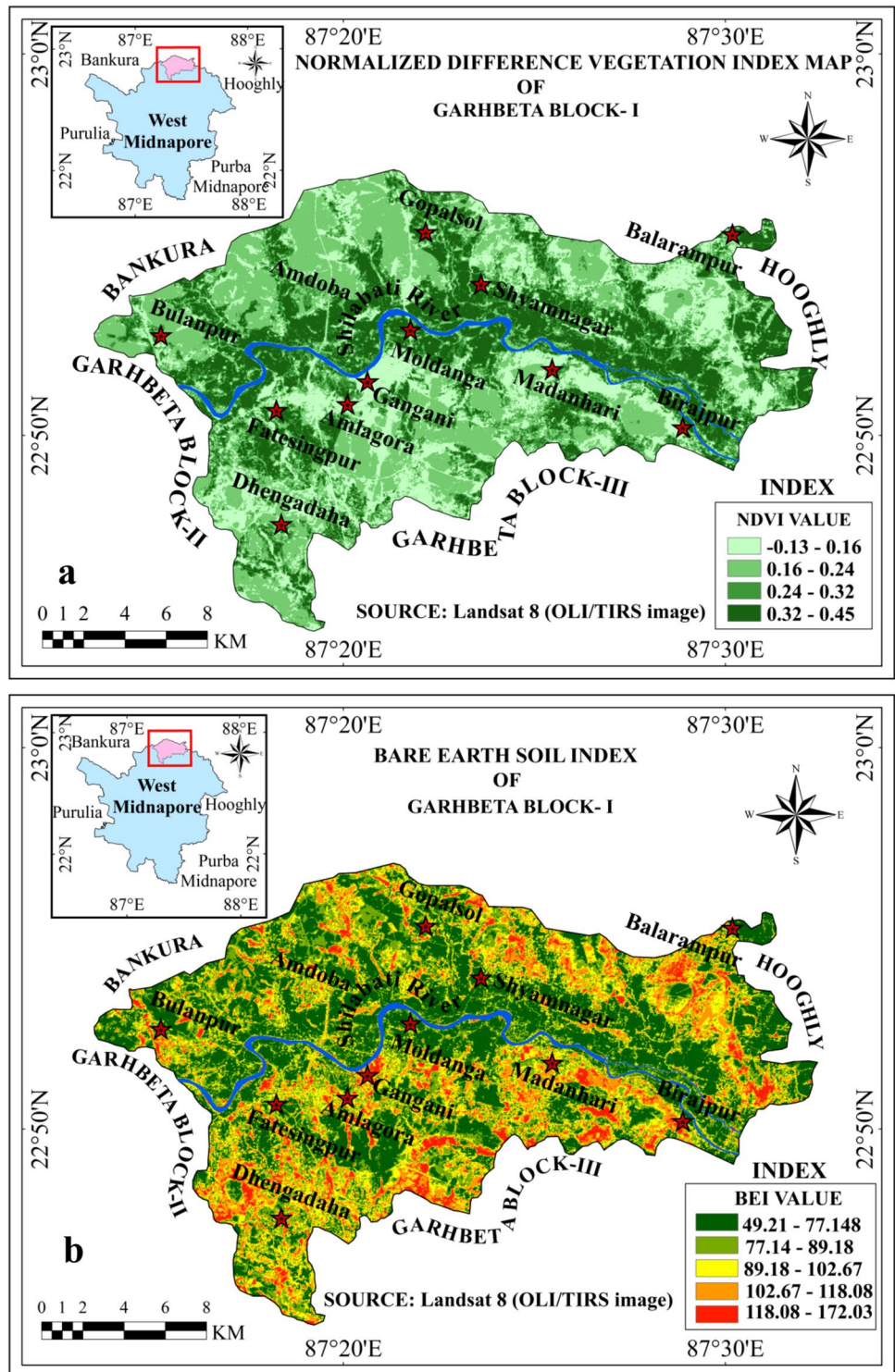
### Relationship between soil loss and spectral indices

The empirical model of soil loss erosion is also validated with a correlation coefficient regression factor into two different indices, namely the Normalized Difference Vegetation Index (NDVI) and the Bare Soil Index (BSI) index. Yang and Shi (1994) developed the empirical model the relationships between soil loss ratios and canopy cover and surface

**Table 7** Annual rate of soil erosion in the study area

Sl No	Soil Erosion hazard Classes	Rate of Soil loss(ton/hect/year)	Area Under affected in Soil erosion	Soil erosion in Land Use & Land cover Classes	Soil erosion Rate in Area hectares	% of Area
1	Low	< 7–8.98	Bulanpur	Plantation of Lateritic Upland	1928.88	5.37
2	Moderate	8.98–10.97	Dhengadaha & Amdoba	Built-upland & Fallow land	5152.63	14.35
3	High	10.97–12.96	Madanhari & Birajpur	Open Forest	6422.4	17.86
4	Very High	12.96–14.95	Moldanga & Shyamnagar	Shrub Land & Agricultural paddy field	8274.69	23.01
5	Extreme	> 14.95–20	Shilabati River Basin area, Gangani, Gopalsol, Amlagora, Fatesingpur	Barren land, Plantation & Agriculture fallow land	11,657.25	32.42

**Fig. 11** Soil loss empirical algorithm (RUSLE) model validated in two indices (a) Normalized Difference Vegetation Index (NDVI) and (b) Bare Earth Soil Index (BESI/BSI)

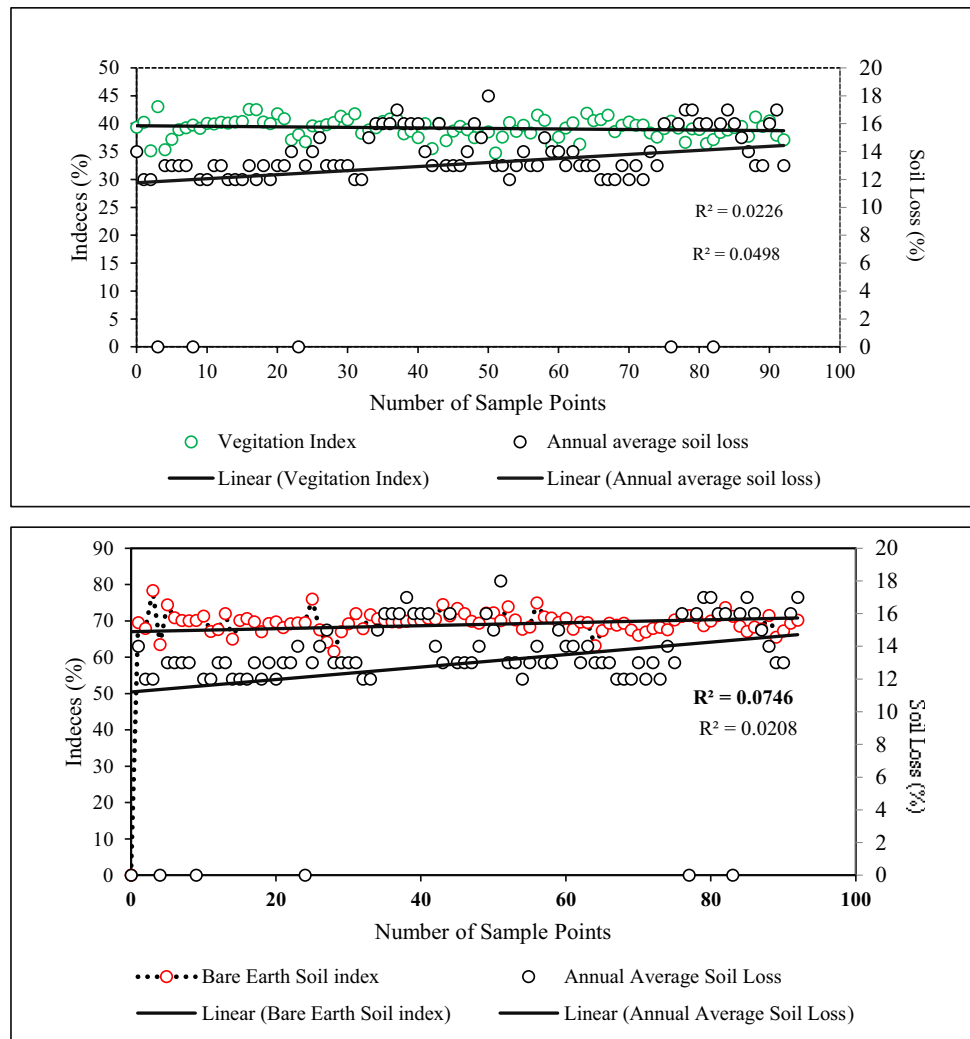


cover sub-factors. However, it is necessary to model validate by using some randomly selected ground truth points. Here are 26 tested GPS ground truth points data and the surrounding 66 training data sets of Google Earth points to estimate the correlation coefficient between NDVI, Bare Soil Index, and Soil erosion rate. Here, we have taken three parameters,

i.e., vegetation index, bare soil index and annual soil loss. In this context, the ‘X’ axis represents the number of ground points of soil loss and the ‘Y’ axis represents the indices values (Fig. 12). It is clearly observed that agricultural land and crop management factors (NDVI) have highly positive correlations ( $R^2 = 0.859$ ,  $RMSE = 0.044$ ) with the annual



**Fig. 12** Statistical regression co-efficient correlation analysis using XLSTAT software; (a) the relationship between NDVI and annual soil loss and, (b) the relationship between BESI/BSI and annual soil loss



average soil loss ( $R^2=0.722$ ). The bare soil index represents the slightly positive correlates ( $R^2=0.841$ ,  $RMSE=0.038$ ) with the annual soil loss ( $R^2=0.722$ ) index due to the effect in sheet/rill erosion by playing a major role in the surface runoff, climatological conditions, surface morphometry, and weathering processes (Physical and Chemical both). Among all three parameters are have a positive relationship (Table 8). In this lateritic area, the bare earth soil index and

NDVI are the most important factors for land management systems that are also related to soil erosion. The present study deals with the soil erosion hazard map by considering abrupt changes in the physical and chemical weathering induced by gully erosion, land use and land cover transformation, flood inundation, and sediment transportation in the river basin areas that directly impact the climate change phenomenon (Fig. 13).

**Table 8** Statistical experiment for evaluate the model validation through co-relationship between three parameters of Annual soil loss rates, NDVI & BSI index in different approaches ( $R^2$  &  $RMSE$ )

Sl No	Soil Erosion hazard Classes	Rate of Soil loss(ton/hect/year)	Soil Loss $R^2$	NDVI Ranges	$R^2$	RMSE	Bare Soil Index(BSI)	Soil Loss $R^2$	$R^2$	RMSE
1	Low	<7–8.98	0.722	<-0.13	0.859	0.044	49.21–77.14	0.722	0.741	0.038
2	Moderate	8.98–10.97		-0.13–0.16			77.14–89.18			
3	High	10.97–12.96		0.16–0.24			89.18–102.67			
4	Very High	12.96–14.95		0.24–0.32			102.67–118.08			
5	Extreme	> 14.95–20		0.32–0.45			118.08172.03			



**Fig. 13** Types of soil erosion in Garhbeta Block-I region in different perspective; (a) Weathering layer of badland topography in Gangani (Surface soils with nodular grains & Duricrust, pisolithic grains with brown color and iron oxide). (b) Rill & Gully erosion in open forest area; (c) Extreme rate of soil erosion in downstream of Shilabati river catchment basin area due to effect of chemical weathering and

sand mining washover processes (Paddy field); (d) Stratigraphic section are decomposed by conglomeratic grains with relative low oxide contain, silica dominated hydrated alumina zone (e) Gulley erosion in undulating badland topography and (f) Experiment and measurement of rill and gullies due to field survey

## Conclusions

The landscape of Gangani is highly dissected by the extension of rills, gullies, and ravines across the lateritic terrain under 40 m elevation of terraced banks along the river Shilabati in Garhbeta Block-I, of Paschim Medinipur District, West Bengal. Deep gullies and ravines have exposed the laterite profiles and underlying depositional facies of sedimentary beds across the badland surface. Land degradation and water-induced soil loss are one of the major criteria of the global and local level environmental problems that threaten the natural ecosystem. The application of the universal soil loss equation model reveals that topsoil of the lateritic upland surface is removed by seasonal runoff in the monsoon months and also by deep weathering processes during the wet period. In the head wards of badland terrain, areas affected by forest loss provide opportunities for rapid surface runoff processes and reduced infiltration rates. The significant duricrust formation is recorded on the top of lateritic terrain after the removal of palythite and exposure to the subaerial conditions under alternate dry and wet conditions. Further, the exposed duricrust layer is weathered and fragmented by local drainage and

climatic conditions. The application of the Revised Universal Soil Loss Equation (RUSLE) Model reveals that topsoil of the lateritic upland surface is removed by seasonal runoff in the monsoon months and also by deep weathering processes during the wet period. The study also reveals about 20 tons/ha/yr of soil, usually removed from the study areas of Garhbeta Block-I, which increases the nutrient loss around the cultivated area.

The present study revealed that to estimate the annual average soil loss (AVSL) and identify the suitable sites for soil erosion hazard prone areas of the Garhbeta Block I. The result of the study focused on the application of the empirical algorithm in the RUSLE model and integrated it with Geographic Information System (GIS) tools to assess soil loss erosion. According to the findings of the study, the mean annual average soil loss estimated in the RUSLE model is nearly 11,657.25 (Soil loss rate > 14.95–20 ton/hectares/year) hectares in the Shilabati river catchment lateritic undulating upland areas of badland topography (agricultural fallow land & barren land); and the built-upland and fallow land have a moderate soil loss probability; indicating that 5152.63 hectares (8.98–10.9720 ton/hectares/year) and a low soil erosion rate (1928.88

hectares) areas are delineated in the downstream (Shilabati River) region, which is covered by plantation and shrubland areas on the upper surface of the badland topography (< 7–8.98 ton/hectares/year). The outcome of the research shows that the very extreme erosion rates are observed in Gangani, Gopalsol, Amlagora, Fatesingpur, Moldanga, Shyamnagar, Madanhari, and Birajpur. Land use and Land Cover (LULC), slope, aspect, and contour patterns as a geomorphological signature, climatological conditions, and crop rotation play a significant role in controlling soil loss, and overgrazing should be prohibited to reduce surface soil loss. Soil erosion is very rapid in the lateritic badlands of the Garhbeta-I Block. There are some natural-based solutions that can be recommended for the reduction of soil erosion in the study area, such as; i) the floor of the badlands is affected by wash deposits and material transport during the monsoonal rains. To increase the moisture retention capacity of the open and bare soil surface, plantation of iron-resistant vegetation (i.e. *Anacardium sp*; and *Mangifera sp*) is needed. At the same time, the humus content may be increased with the deposition of litter and growth of grasses below the planted trees, which may resist the surface runoff induced erosion in the lateritic floor. ii) the gully banks with sandy alluviums may be used for plantation of vetiver grasses (*Vetiveria zizanioides*) with modification of slopes and bio-engineered surfaces to protect the bank recession during the wet season. The promotion of bio-engineered bank margins with the plantation of grasses can minimize the soil losses with time, and iii). the valley across the check dam with the local materials block the sudden flow of water along the gully channel to reduce the flow energy and erosion along the valley floor. Thus, the above management practises will reduce the soil erosion from the different sources of lateritic river banks along the Shilabati river basin in Garhbeta- Block-I. The planner should be implemented by policymakers for managing soil erosion hazards in the most efficient manner in the Shilabati basin for treatment of plantation strategies and, land use and land management practices.

**Abbreviations** RUSLE: Revised universal soil loss equation; AVSL: Annual average soil loss; USGS: United States geological survey; IMD: Indian metrological department; NBSS: National Bureau of soil survey and land use planning; SOI: Survey of India; GSI: Geological Survey of India; DEM: Digital elevation model; OLI: Operational land imager; TIRS: Thermal infrared sensor; NDVI: Normalized difference vegetation index; BSI: Bare soil index; LULC: Land use & land cover; CMF: Crop management factor; SPF: Support practice factor; IDW: Inversed distance weight; RMSE: Root mean square error; USDA: United States Department of Agriculture; AAP: Average annual precipitation; GIS: Geographic information system; SEF: Soil erodibility factor; EUROSEM: European soil erosion model; LISEM: Limburg soil erosion model; USLE: Universal soil loss equation; SWAT: Soil & water assessment tool; WEPP: Water erosion prediction project; REF: Rainfall erosivity factor

**Acknowledgements** All authors would like to acknowledge in the Department of Remote Sensing and GIS, Vidyasagar University for continuously supporting laboratory uses and conducting the extensive field survey of this work. The authors would like to thank Subhankar Naskar, Kushal Nayak, Soumen Dey, and Dipu Kauri for helping during the field survey. We would like to express our sincere thanks to USGS Earth Explorer, Bhuvan-NRSC, GSI, NBSS&LUP and all Government organizations for data supporters and all websites.

**Data availability statements** All data generated or analysed during this study are included in this published article (and its supplementary information files).

## Declarations

**Conflict of interest** The all authors declared that they have no conflict of interest.

## References

- Agele DM, Lihan TB, Rahim SA, Rahman ZA (2013) Risk assessment of soil erosion downstream of the Pahang river basin with RUSLE model. *Res Gate* 19(2):571–580
- Angima SD, Stott DE, O’neill MK, Ong CK, Weesies GA (2003) Soil erosion prediction using RUSLE for central Kenyan highland conditions. *Agr Ecosyst Environ* 97(1–3):295–308. [https://doi.org/10.1016/S0167-8809\(03\)00011-2](https://doi.org/10.1016/S0167-8809(03)00011-2)
- Arnold JG, Fohrer N (2005) SWAT2000: current capabilities and research opportunities in applied watershed modelling. *Hydrol Process Int J* 19(3):563–572. <https://doi.org/10.1002/hyp.5611>
- Atoma H, Suryabhagavan KV, Balakrishnan M (2020) Soil erosion assessment using RUSLE model and GIS in Huluka watershed, Central Ethiopia. *Sustain Water Resour Manag* 6(1):1–17. <https://doi.org/10.1007/s40899-020-00365-z>
- Balasubramani K, Veena M, Kumaraswamy K, Saravanabavan V (2015) Estimation of soil erosion in a semi-arid watershed of Tamil Nadu (India) using revised universal soil loss equation (rusle) model through GIS. *Model Earth Syst Environ* 1(3):10. <https://doi.org/10.1007/s40808-015-0015-4>
- Becker F, Choudhury BJ (1988) Relative sensitivity of normalized difference vegetation index (NDVI) and microwave polarization difference index (MPDI) for vegetation and desertification monitoring. *Remote Sens Environ* 24(2):297–311. [https://doi.org/10.1016/0034-4257\(88\)90031-4](https://doi.org/10.1016/0034-4257(88)90031-4)
- Benkobi L, Trlica M, Smith J (1994) Evaluation of a redefined surface cover sub-factor for use in RUSLE. *J Range Manag* 47:74–78. <https://doi.org/10.2307/4002845>
- Bewket W, Teferi E (2009) Assessment of soil erosion hazard and prioritization for treatment at the watershed level: case study in the Chemoga watershed, Blue Nile basin, Ethiopia. *Land Degrad Dev* 20(6):609–622. <https://doi.org/10.1002/ldr.944>
- Bhattarai R, Dutta D (2007) Estimation of soil erosion and sediment yield using GIS at catchment scale. *Water Resour Manage* 21(10):1635–1647. <https://doi.org/10.1007/s11269-006-9118-z>
- Biswas SS, Pani P (2015) Estimation of soil erosion using RUSLE and GIS techniques: a case study of Barakar River basin, Jharkhand, India. *Model Earth Syst Environ* 1(4):42. <https://doi.org/10.1007/s40808-015-0040-3>
- Brady NC, Weil RC (2012) *The nature and properties of soils*. Pearson education, New Delhi



- Chang K-t (2018) Introduction to Geographic Information System, Publisher: McGraw-Hill ISBN: 978-0-07-310171-2
- Chen W, Liu L, Zhang C, Wang J, Wang J, Pan Y (2004) Monitoring the seasonal bare soil areas in Beijing using multitemporal TM images. In IGARSS 2004. 2004 IEEE International Geoscience and Remote Sensing Symposium. IEEE, vol. 5, pp. 3379–3382
- Dabral PP, Baithuri N, Pandey A (2008) Soil erosion assessment in a hilly catchment of North Eastern India using USLE, GIS and remote sensing. *Water Resour Manage* 22(12):1783–1798. <https://doi.org/10.1007/s11269-008-9253-9>
- De Roo APJ, Wesseling CG, Ritsema CJ (1996) LISEM: a single-event physically based hydrological and soil erosion model for drainage basins. I: theory, input and output. *Hydrol Process* 10(8):1107–1117. [https://doi.org/10.1002/\(SICI\)1099-1085\(199608\)10:8%3C1107::AID-HYP415%3E3.0.CO;2-4](https://doi.org/10.1002/(SICI)1099-1085(199608)10:8%3C1107::AID-HYP415%3E3.0.CO;2-4)
- Dunn M, Hickey R (1998) The effect of slope algorithms on slope estimates within a GIS. *Cartography* 27(1):9–15. <https://doi.org/10.1080/00690805.1998.9714086>
- Flanagan DC, Gilley JE, Franti TG (2007) Water Erosion Prediction Project (WEPP): Development history, model capabilities, and future enhancements. *Trans ASABE* 50(5):1603–1612
- Fu G, Chen S, McCool DK (2006) Modeling the impacts of no-till practice on soil erosion and sediment yield with RUSLE, SEDD, and ArcView. *GIS Soil Tillage Res* 85:38–49. <https://doi.org/10.1016/j.still.2004.11.009>
- Gallart F, Marignani M, Perez-Gallego N, Santi E, Maccherini S (2013) Thirty years of studies on badlands, from physical to vegetational approaches. A succinct review. *Catena* 106:4–11. <https://doi.org/10.1016/j.catena.2012.02.008>
- Ganasri BP, Ramesh H (2016) Assessment of soil erosion by RUSLE model using remote sensing and GIS-A case study of Nethravathi Basin. *Geosci Front* 7(6):953–961. <https://doi.org/10.1016/j.gsf.2015.10.007>
- Gitas IZ, Douros K, Minakou C, Silleos GN, Karydas CG (2009) Multi-temporal soil erosion risk assessment in N. Chalkidiki using a modified USLE raster model. *EARSeL eProceedings* 8(1):40–52
- Grimshaw RG, Faiz A (1995) Vetiver grass: application for stabilization of structures. In Proceedings of the Sixth International Conference on Low-Volume Roads (pp. 74–81)
- Gunawan G, Sutjningsih D, Soeryantono H, Sulistioweni S (2013) Soil erosion estimation based on GIS and remote sensing for supporting integrated water resources conservation management. *Int J Tecnol* 4(2):157–166. <https://doi.org/10.14716/ijtech.v4i2.110>
- Hurni H (1985) Soil conservation manual for Ethiopia. Ministry of Agriculture, Addis Ababa
- Jain MK, Kothyari UC (2000) Estimation of soil erosion and sediment yield using GIS. *Hydrol Sci J* 45(5):771–786. <https://doi.org/10.1080/02626660009492376>
- Joshi V, Nagare V (2009) Land use change detection along the Pravara river basin in Maharashtra, using remote sensing and GIS techniques. *Acta Geographica Debrecina Landsc Environ* 3(2):71–86. <https://ojs.lib.unideb.hu/landsenv/article/view/2269>. Accessed 31 Dec 2009
- Kaltenrieder J (2007) Adaption and Validation of the Universal Soil Loss Equation (USLE) for the Ethiopian-Eritrean Highlands (MSc Thesis). Philosophisch-naturwissenschaftliche Fakultät, University of Bern, Bern
- Karaburun A (2010) Estimation of C factor for soil erosion modeling using NDVI in Buyukcekmece watershed. *Ozean J Appl Sci* 3(1):77–85
- KICT (1992) The development of selection standard for calculation method of unit sediment yield in rivers. KICT 89-WR-113
- Kim JB, Saunders P, Finn JT (2005) Rapid assessment of soil erosion in the Rio Lempa Basin, Central America, using the universal soil loss equation and geographic information systems. *Environ Manage* 36(6):872–885. <https://doi.org/10.1007/s00267-002-0065-z>
- Kim JP (1992) Development of optimum facility system for high-rise apartments (II). Report of KICT, 91
- Markose VJ, Jayappa KS (2016) Soil loss estimation and prioritization of sub-watersheds of Kali River basin, Karnataka, India, using RUSLE and GIS. *Environ Monit Assess* 188(4):1–16. <https://doi.org/10.1007/s10661-016-5218-2>
- McCool DK, Brown LC, Foster GR (1987) Revised slope steepness factor for the Universal Soil Loss Equation. *Trans ASAE* 30:1387–1396. <https://doi.org/10.13031/2013.30576>
- Mekuriaw A, Heinimann A, Zeleke G, Hurni H (2018) Factors influencing the adoption of physical soil and water conservation practices in the Ethiopian highlands. *Int Soil Water Conserv Res* 6(1):23–30. <https://doi.org/10.1016/j.iswcr.2017.12.006>
- Miheretu BA, Yimer AA (2018) Estimating soil loss for sustainable land management planning at the Gelana sub-watershed, northern highlands of Ethiopia. *Int J River Basin Manag* 16(1):41–50. <https://doi.org/10.1080/15715124.2017.1351978>
- Millward AA, Mersey JE (1999) Adapting the RUSLE to model soil erosion potential in a mountainous tropical watershed. *CATENA* 38(2):109–129. [https://doi.org/10.1016/S0341-8162\(99\)00067-3](https://doi.org/10.1016/S0341-8162(99)00067-3)
- Moore ID, Burch GJ (1986) Physical basis of the length-slope factor in the Universal Soil Loss Equation. *Soil Sci Soc Am J* 50(5):1294–1298. <https://doi.org/10.2136/sssaj1986.036159950050000500042x>
- Morgan RPC, Quinton JN, Smith RE, Govers G, Poesen JWA, Auerswald K, Styczen ME (1998) The European Soil Erosion Model (EUROSEM): a dynamic approach for predicting sediment transport from fields and small catchments. *Earth Surf Process Landforms* 23(6):527–544. [https://doi.org/10.1002/\(SICI\)1096-9837\(199806\)23:6%3C527::AID-ESP868%3E3.0.CO;2-5](https://doi.org/10.1002/(SICI)1096-9837(199806)23:6%3C527::AID-ESP868%3E3.0.CO;2-5)
- Nadal-Romero E, Murillo JFM, Kuhn NJ (Eds) (2018) Badlands Dynamics in a Context of Global Change. Elsevier
- Naqvi HR, Mallick J, Devi LM, Siddiqui MA (2013) Multi-temporal annual soil loss risk mapping employing revised universal soil loss equation (RUSLE) model in Nun Nadi Watershed, Uttarakhand (India). *Arab J Geosci* 6(10):4045–4056. <https://doi.org/10.1007/s12517-012-0661-z>
- Narayana DV, Babu R (1983) Estimation of soil erosion in India. *J Irrig Drain Eng* 109(4):419–434. [https://doi.org/10.1061/\(ASCE\)0733-9437\(1985\)111:4\(408\)](https://doi.org/10.1061/(ASCE)0733-9437(1985)111:4(408))
- Nguyen CT, Chidthaisong A, Kieu Diem P, Huo LZ (2021) A modified bare soil index to identify bare land features during agricultural fallow-period in southeast Asia using Landsat 8. *Land* 10(3):231. <https://doi.org/10.3390/land10030231>
- Nyssen J, Veyret-Picot M, Poesen J, Moeyersons J, Haile M, Deckers J, Govers G (2004) The effectiveness of loose rock check dams for gully control in Tigray, northern Ethiopia. *Soil Use Manag* 20(1):55–64. <https://doi.org/10.1111/j.1475-2743.2004.tb00337.x>
- Okon PB, Babalola O (2004) General variability of soils under Vetiver grass strips: focus on combating land and environmental degradation. *Vetiver Netw* 17(4):1–10
- Pal SC, Shit M (2017) Application of RUSLE model for soil loss estimation of Jaipanda watershed, West Bengal. *Spatial Inf Res* 25(3):399–409. <https://doi.org/10.1007/s41324-017-0107-5>
- Pandey A, Chowdary VM, Mal BC (2007) Identification of critical erosion prone areas in the small agricultural watershed using USLE, GIS and remote sensing. *Water Resour Manage* 21(4):729–746. <https://doi.org/10.1007/s11269-006-9061-z>
- Panditharathne DLD, Abeysingha NS, Nirmanee KGS, Mallawatantri A (2019) Application of revised universal soil loss equation (Rusle) model to assess soil erosion in “kalu Ganga” River Basin in Sri Lanka. *Appl Environ Soil Sci* 2019. <https://doi.org/10.1155/2019/4037379>



- Paul AK (2002) Coastal geomorphology and environment. ACB Publication, Kolkata, pp 1–342
- Pérez-Rodríguez R, Marques MJ, Bienes R (2007) Spatial variability of the soil erodibility parameters and their relation with the soil map at subgroup level. *Sci Total Environ* 378(1–2):166–173. <https://doi.org/10.1016/j.scitotenv.2007.01.044>
- Pimentel D, Allen J, Beers A, Guinand L, Linder R, McLaughlin P, Siebert S (1987) World agriculture and soil erosion. *Bioscience* 37(4):277–283. <https://doi.org/10.2307/1310591>
- Poesen J, Nachtergaele J, Verstraeten G, Valentin C (2003) Gully erosion and environmental change: importance and research needs. *CATENA* 50:91–133. [https://doi.org/10.1016/S0341-8162\(02\)00143-1](https://doi.org/10.1016/S0341-8162(02)00143-1)
- Prasannakumar V, Shiny R, Geetha N, Vijith HJEES (2011) Spatial prediction of soil erosion risk by remote sensing, GIS and RUSLE approach: a case study of Siruvani river watershed in Attapady valley, Kerala, India. *Environ Earth Sci* 64(4):965–972. <https://doi.org/10.1007/s12665-011-0913-3>
- Rao Y (1981) Evaluation of cropping management factor in universal soil loss equation under natural rainfall condition of Kharagpur, India. Bangkok, Proceedings of the Southeast Asian Regional Symposium on Problems of Soil Erosion and Sedimentation, Asian Institute of Technology (AIT), (p. 241–254)
- Renard KG (1997) Predicting soil erosion by water: a guide to conservation planning with the Revised Universal Soil Loss Equation (RUSLE). United States Government Printing
- Renard KG, Foster GR, Weesies GA, Porter JP (1991) RUSLE: Revised universal soil loss equation. *J Soil Water Conserv* 46(1):30–33. <https://www.jswnonline.org/content/46/1/30>. Accessed Jan 1991
- Renard KG, Foster GR, Weesies GA, McCool DK, Yoder DC (1996) Predicting soil erosion by water: a guide to conservation planning with the revised universal soil loss equation (RUSLE). Handbook No. 703. USDA Agricultural, Washington, DC
- Renard KG, Freid JR (1994) Using monthly precipitation data to estimate the R factor in the revised USLE. *J Hydrol* 157:287–306. [https://doi.org/10.1016/0022-1694\(94\)90110-4](https://doi.org/10.1016/0022-1694(94)90110-4)
- Robert PS, Hilborn D (2000) Factsheet: universal soil loss equation (USLE). &nbsp;Index No-572/751, Queen's printer for Ontario, 35–36
- Rouse JW, Haas RH, Schell JA, Deering DW (1974) Monitoring vegetation systems in the Great Plains with ERTS. NASA Special Publication 351(1974): 309
- Simms AD, Woodroffe CD, Jones BG (2003) Application of RUSLE for erosion management in a coastal catchment, southern NSW
- Singh G, Panda RK (2017) Grid-cell based assessment of soil erosion potential for identification of critical erosion prone areas using USLE, GIS and remote sensing: a case study in the Kapgari watershed, India. *Int Soil Water Conserv Res* 5(3):202–211. <https://doi.org/10.1016/j.iswcr.2017.05.006>
- Sinha D, Joshi VU (2012) Application of universal soil loss equation (USLE) to recently reclaimed badlands along the Adula and Mahalungi Rivers, Pravara Basin, Maharashtra. *J Geol Soc India* 80(3):341–350
- Stillhardt B, Herweg KG, Hurni H (2002) Long-term monitoring of soil erosion and soil and water conservation in Afdeyu, Eritrea (1984–1998): Soil erosion and soil and water conservation database. Centre for Development and Environment.
- Tripathy BK, Panda T, Mohanty RB (2014) Traditional artifacts from Bena grass [*Chrysopogon zizanioides* (L.) Roberty] (Poaceae) in Jajpur district of Odisha, India. *Indian J Tradit Knowl* 13(4):771–777
- Udayakumara EPN, Shrestha RP, Samarakoon L, Schmidt-Vogt D (2010) People's perception and socioeconomic determinants of soil erosion: a case study of Samanlalawewa watershed, Sri Lanka. *Int J Sedim Res* 25(4):323–339. [https://doi.org/10.1016/S1001-6279\(11\)60001-2](https://doi.org/10.1016/S1001-6279(11)60001-2)
- Ustun B (2008) Soil erosion modelling by using GIS and remote sensing: a case study Ganos Mountain. *Int Arch Photogramm Remote Sens Spat Inf Sci* 37:1681–1684. [https://www.isprs.org/proceedings/XXXVII/congress/7\\_pdf/10\\_ThS-18/26.pdf](https://www.isprs.org/proceedings/XXXVII/congress/7_pdf/10_ThS-18/26.pdf). Accessed 3–11 Jul 2008
- Van der Knijff JM, Jones RJA, Montanarella L (2000) Soil erosion risk: assessment in Europe. ERU 19044 EN. Office for Official Publications of the European Communities, Luxembourg, p 34. [https://www.unisdr.org/files/1581\\_ereurnew2.pdf](https://www.unisdr.org/files/1581_ereurnew2.pdf). Accessed 2000
- Valentin C, Poesen J, Li Y (2005) Gully erosion: impacts, factors and control. *CATENA* 63:132–153. <https://doi.org/10.1016/j.catena.2005.06.001>
- Wang G, Gertner G, Fang S, Anderson AB (2003) Mapping multiple variables for predicting soil loss by geostatistical methods with TM images and a slope map. *Photogramm Eng Remote Sens* 69(8):889–898. <https://doi.org/10.14358/PERS.69.8.889>
- Wen L, Zheng F, Shen H, Bian F, Jiang Y (2015) Rainfall intensity and inflow rate effects on hillslope soil erosion in the Mollisol region of Northeast China. *Nat Hazards* 79(1):381–395. <https://doi.org/10.1007/s11069-015-1847-y>
- Wijesundara NC, Abeysingha NS, Dissanayake DMSLB (2018) GIS-based soil loss estimation using RUSLE model: A case of Kirindi Oya river basin, Sri Lanka. *Model Earth Syst Environ* 4(1):251–262. <https://doi.org/10.1007/s40808-018-0419-z>
- Wischmeier WH, Smith DD (1978) Predicting rainfall erosion losses: a guide to conservation planning (No. 537). Department of Agriculture, Science and Education Administration. [http://topsoil.nserl.purdue.edu/usle/AH\\_537.pdf](http://topsoil.nserl.purdue.edu/usle/AH_537.pdf). Accessed Dec 1978
- Xu YQ, Zhou QF, Li SC (2005) An analysis on spatial–temporal distribution of rainfall erosivity in Guizhou Province. *Bull Soil Water Conserv* 4:11–14
- Yang IT, Shin KJ, Kim DM, Yu YG (1999) Prediction of soil loss in watershed using universal soil loss equation and Geo-spatial Information System. *J Ind Technol* 19:147–154
- Yang D, Kanae S, Oki T, Koike T, Musiak K (2003) Global potential soil erosion with reference to land use and climate changes. *Hydrol Process* 17(14):2913–2928. <https://doi.org/10.1002/hyp.1441>
- Yang Y, Shi D (1994) Study on Soil Erosion in the Three Gorge Area of the Changjiang River
- Yinglun S (2018) Fiji introduces Vetiver system to deal with soil erosion. Xinhua News Agency, 21 September, 2018, p. 1
- Yue-Qing X, Xiao-Mei S, Xiang-Bin K, Jian P, Yun-Long C (2008) Adapting the RUSLE and GIS to model soil erosion risk in a mountains karst watershed, Guizhou Province, China. *Environ Monit Assess* 141(1–3):275–286. <https://doi.org/10.1007/s10661-007-9894-9>
- Zeitl, C. (2015) Vetiver grass for soil and moisture conservation. Inputs for the Technology Core Group of Kigali Entry Project. Rapid Planning. Retrieved from [https://www.ifeu.org/nachhaltigkeit/pdf/G6\\_IFEU\\_140816\\_Vetiver%20grass%20for%20soil%20and%20moisture%20conservation.pdf](https://www.ifeu.org/nachhaltigkeit/pdf/G6_IFEU_140816_Vetiver%20grass%20for%20soil%20and%20moisture%20conservation.pdf). Accessed 20 Jan 2021
- Zhou P, Luukkanen O, Tokola T, Nieminen J (2008) Effect of vegetation cover on soil erosion in a mountainous watershed. *CATENA* 75(3):319–325. <https://doi.org/10.1016/j.catena.2008.07.010>